# Modelling carbofuran biotransformation by *Novosphingobium* sp. KN65.2 in the presence of coincidental carbon and indigenous microbes

*Li Liu[1,2†], Damian E. Helbling[3,4*†], Hans-Peter E. Kohler[3], Barth F. Smets[1]**

[1]Department of Environmental Engineering, Technical, University of Denmark, Bygningstorvet 115, 2800 Kgs.Lyngby, Denmark;

[2]School of Chemistry, Beihang University, Beijing 100191, P. R. China;

[3]Eawag, Swiss Federal Institute of Aquatic Science and Technology, Department of Environmental Microbiology, Überlandstrasse 133, 8600 Dübendorf, Switzerland;

[4]School of Civil and Environmental Engineering, Cornell University, Ithaca, NY, USA.

***Corresponding authors:**

bfsm@env.dtu.dk, phone: +45 45 25 22 30, fax: +45 45 93 28 50

damian.helbling@cornell.edu, phone: +1 607 255 5146, fax: +1 607 255 9004

**†These authors contributed equally to this work**

This document is the accepted manuscript version of the following article:
Liu, L., Helbling, D. E., Kohler, H. P. E., & Smets, B. F. (2019). Modelling carbofuran biotransformation by: Novosphingobium sp. KN65.2 in the presence of coincidental carbon and indigenous microbes. Environmental Science: Water Research and Technology, 5(4), 798-807. https://doi.org/10.1039/c8ew00929e

20 **Abstract Art**

21 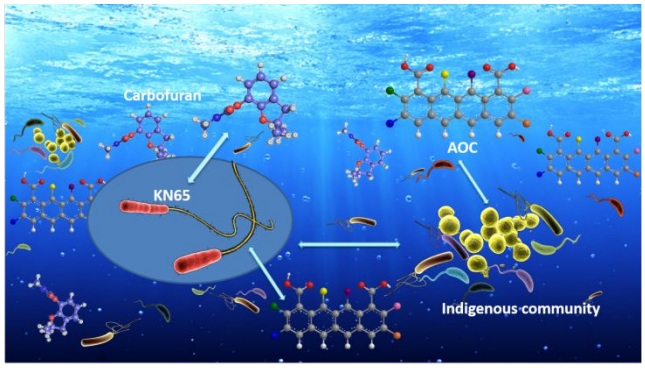

## ABSTRACT

The influence that coincidental carbon substrates (i.e., assimilable organic carbon, AOC) and indigenous microbial communities has on pesticide biotransformation by degrader strains in aquatic environments is poorly understood. We conducted batch experiments to investigate carbofuran biotransformation by *Novosphingobium* sp. KN65.2 using four environmentally derived water samples with varying amounts and types of AOC and indigenous microbial communities. We designed experimental scenarios to explore the influence of AOC and indigenous microbial communities on the growth of strain KN65.2 and the biotransformation of carbofuran. Relevant kinetic parameters were estimated from simpler experiments, and used to predict the growth of strain KN65.2 and the biotransformation of carbofuran in more complex experiments with an additive biokinetic model. We found that our additive biokinetic model adequately predicts the growth of strain KN65.2 and the rate of carbofuran biotransformation in natural waters that support the growth of strain KN65.2. However, our model over-predicts the growth of strain KN65.2 and the rate of carbofuran biotransformation in low-AOC environments. Overall, our results define the scope within which additive biokinetic models can be used to predict pesticide biotransformation in the presence of coincidental carbon substrates and indigenous microbial communities.

## INTRODUCTION

The presence of pesticides in aquatic systems, even at trace concentrations (ng-$\mu$g $L^{-1}$ range), might pose long-term environmental or human health risks.[1-3] Many pesticides are inherently biodegradable; one option to accelerate the removal of pesticides from contaminated water systems is through the addition of bacterial strains with metabolic capabilities to mineralize certain types of pesticides.[4, 5] This process is known as bio-augmentation,[6] and bio-augmentation might happen in a distributed (e.g., addition to aquifers) or localized (e.g., addition to unit processes in water treatment facilities) manner.[7, 8] The practice of bio-augmentation has, however, often failed or is only briefly successful.[9] One likely reason for this failure is that pesticide degrading strains are enriched and isolated at high pesticide concentrations and they cannot handle substrates at low concentrations.[10] In addition to the physiological challenges presented when growth substrates are present at trace concentrations,[11] there are at least two other fundamental considerations that have rarely been explored when evaluating pesticide bio-augmentation scenarios. First, natural water systems contain assimilable organic carbon (AOC) consisting of a complex mixture of substrates in addition to trace-levels of pesticides.[12, 13] The presence of AOC, which we refer to as coincidental carbon substrates, supports the growth of indigenous microbial communities and may or may not support the growth of the added pesticide degrader. It is also unclear whether the presence of AOC, typically at higher concentrations than the pesticide in question, would result in physiological changes in pesticide degraders and could lead to the down regulation of relevant pesticide catabolic pathways.[14-16] Second, natural waters contain indigenous microbial communities, and their presence can be a key factor for pesticide biodegradation. For example, indigenous microbial communities might compete for AOC or other essential nutrients and affect the density and fate of the pesticide degraders.[17, 18]

To the best of our knowledge, the literature lacks reports on growth measurements of specific pesticide degraders with concomitant measurements of pesticide biodegradation at low concentrations *in the presence* of AOC and indigenous microbial communities. We believe it is essential to understand and describe, using suitable models, the interactions between AOC and indigenous microbial communities and pesticide degradation in aquatic environments. Such knowledge would allow us to predict potential failure and success of bio-augmentation strategies for pesticide removal from aquatic systems. Complementary approaches, based on partial least square analysis, have been examined to predict strain survival and biodegradation activity in contaminated soils based on soil physico-chemical soil characteristics.[19] In this work, we studied the removal of the carbamate insecticide carbofuran by *Novosphingobium* sp. KN65.2, a strain that can mineralize carbofuran as the sole carbon source[5] in batch experiments with increasing complexity. We conducted the experiments using water derived from a variety of natural sources that contained varying amounts and types of AOC. Experiments were conducted to explicitly measure growth of strain KN65.2 on AOC in the absence of an indigenous microbial community, growth of the indigenous microbial community on AOC in the absence of strain KN65.2, growth of strain KN65.2 on AOC and carbofuran in the absence of an indigenous microbial community, and growth of both the indigenous microbial community and strain KN65.2 on AOC and carbofuran. In the latter two cases, we also measured carbofuran biotransformation. In previous work, we measured growth and carbofuran utilization kinetics of KN65.2 in the absence of AOC.[10] We also previously introduced an additive biokinetic model framework to describe growth-linked biodegradation of trace-level pollutants in the presence of coincidental carbon substrates and indigenous microbial communities, which we tentatively validated against limited literature-reported experimental data.[20] The dataset generated by the experiments reported here allows for a

more thorough evaluation of the proposed biokinetic model, which facilitates a full interpretation of the experimental results and leads to generalizable insights on the fundamentals of trace-level pesticide degradation in natural systems.

## MATERIALS AND METHODS

**Carbofuran and strain KN65.2.** We selected carbofuran as the model pesticide because it is frequently measured in surface and groundwater resources[21-26] and its occurrence in drinking water is regulated around the world.[27] We purchased carbofuran (99.9% purity) from Sigma-Aldrich (Seelze, Germany) and prepared spike solutions in AOC-restricted mineral medium at 100 mg $L^{-1}$ as previously described.[10] *Novosphingobium* sp. strain KN65.2 has the ability to mineralize carbofuran, and the biotransformation pathway is initiated by carbamate hydrolysis.[5] We received strain KN65.2 as a streak on an R2A agar plate from D. Springael *(Department of Earth and Environmental Sciences, KU Leuven).* A single colony was picked from the agar plate and added to 5 mL of sterilized LB medium. Cells were grown to early-stationary phase and diluted to approximately 15 % glycerol (0.5 mL of 50 % sterile glycerol added to 1 mL cell culture) and stored at -80 °C.

**Environmental water samples.** We collected water from four sources: groundwater (GW); bank filtrate (BF); shallow stream (SS); and stagnant pond (SP) near Dübendorf (CH). We reasoned that each of the water samples would contain varying quantities and qualities of AOC and diverse indigenous microbial communities. The samples were collected in 2 L trace clean glass bottles and pasteurized (30 min at 60°C) within 30 minutes of sampling as previously described.[10] A sufficient volume of each sample was preserved without pasteurization to allow for subsequent re-inoculation of the indigenous microbial community. All water samples were characterized for

dissolved organic carbon (DOC), specific UV absorbance (SUVA), pH, and specific conductivity following standard procedures.[28]

**Batch Experiments.** All glassware and caps used for batch experiments were treated rigorously to remove any residual AOC as previously described.[17, 29] Aliquots of 20 mL of the pasteurized water samples were filtered through a 0.1 µm Millex® syringe filter (Millipore, Billerica, MA, USA) into a 40 mL borosilicate glass vial. The 0.1 µm Millex® syringe filter was selected to ensure that all microorganisms were removed and to limit the leaching of AOC from the filters into the samples; the small pore size may have removed a negligible amount of larger AOC constituents. The borosilicate glass vials were again pasteurized (30 min at 60°C) to ensure sterile conditions. We designed four experimental scenarios to meet the project objectives (See Fig 1 in [20]). *First*, the indigenous microbial community was re-introduced into three vials at a concentration of $10^3$ cells $mL^{-1}$ and growth on the residual AOC was measured by flow cytometry. The inoculum was derived from unpasteurized water samples and cells in the inoculum were quantified by means of flow cytometry. *Second*, strain KN65.2 was spiked into three vials at a concentration of $10^3$ cells $mL^{-1}$ and growth on the residual AOC was measured by flow cytometry. The inoculum was prepared from the frozen glycerol stock and grown in mineral medium amended with approximately 10 mg $L^{-1}$ of carbofuran as previously described;[10] cells were washed in mineral medium three times to remove any residual AOC prior to inoculation in experiments. *Third*, strain KN65.2 was spiked into three vials at a concentration of $10^3$ cells $mL^{-1}$ along with 1 mg $L^{-1}$ of carbofuran. Growth of strain KN65.2 on residual AOC plus carbofuran was measured by flow cytometry and carbofuran biotransformation was measured by HPLC-UV. *Fourth*, the indigenous microbial community and strain KN65.2 were both added to three vials at a concentration of $10^3$ cells $mL^{-1}$ along with 1 mg $L^{-1}$ of carbofuran. Growth of the combined microbial community on

residual AOC and carbofuran was measured by flow cytometry, growth of strain KN65.2 was inferred from qPCR-based detection of KN65.2 in total community DNA extracts, and carbofuran biotransformation was measured by HPLC-UV. All batch experiments were conducted at 30 °C. Samples were taken at the time of inoculation and periodically thereafter until cell density measurements suggested stationary phase or carbofuran concentration was below the limit of detection (<0.05 mg $L^{-1}$).

**Quantification of growth by flow cytometry.** Cell densities were measured on a BD Accuri C6 Flow Cytometer (Erembodegem, Belgium). Aliquots of 500 µL from a batch experiment were combined with 5 µL of SYBR Green stain (Molecular Probes, Ba 154 sel, Switzerland) diluted 100-fold in dimethylsulfoxide (Fluka Chemie AG, Buchs, Switzerland) in a 1.5 mL plastic centrifuge tube (Greiner Bio One, Frickenhausen, Germany), vortexed briefly, and incubated in the dark at 40 ºC for 10 minutes. For cell densities less than $5 \times 10^5$ cells $mL^{-1}$, samples were measured directly on the BD Accuri C6 Flow Cytometer without dilution; for cell densities greater than $5 \times 10^5$ cells $mL^{-1}$, samples were diluted in filter-sterilized water. Data were analyzed with the CFlow v1.0.227.4 flow cytometry software. Enumeration was achieved with signals collected on the gated combined 533 nm/670nm density plot as previously described.[30]

**Quantification of carbofuran biotransformation.** HPLC-UV analyses were performed on a Gynkotek system with a Dionex ASI-100 autosampler and a UVD 340U diode array detector. Carbofuran was separated on a Nucleosil 100-5 C18 HD column (250×4.0 mm) with an octadecyl modified high density silica stationary phase (Macherey-Nagel, Düren, Germany). The HPLC was operated isocratically at a flow rate of 0.7 mL $min^{-1}$ with 55 % methanol and 45 % nanopure water eluents. Limits of quantification for carbofuran were less than 0.05 mg $L^{-1}$ with a 50 µL injection volume. The Chromeleon Client v6.6 (Dionex) was used for chromatogram analysis.

**Quantification of growth of strain KN65.2 by means of qPCR.** The collected cells were subject to DNA extraction using the MP FastDNA™ SPIN Kit (MP Biomedicals LLC., Solon, USA) following manufacturer's instructions. Concentration and purity of extracted DNA were checked by spectrophotometry (NanoDrop Technologies, Wilmington, DE, USA). qPCR was carried out on extracted DNA samples to determine the relative abundance of KN65.2 cells based on the *cfdC* gene and the 16S rRNA gene as targets for quantification of KN65.2 and all bacteria, respectively. For *cfdC* detection, primers $cfdC_{for}$: CCGCTCATGCCGTTTATCTAC and $cfdC_{rev}$: GGTTTCCAGATCGAACTCGC, were used with a PCR program consisting of an initial 5 min. denaturation at 94°C, 35 cycles of (94°C: 30 s; 54°C: 20 s; 72°C: 30 s) and final 5 min at 72°C. A unique product size was 252 bp, with melting at 87-88 °C. An *E. coli* clone carrying a *BamHI* fragment of the *cfdC* gene served as source for calibration curves. The *cfdC* qPCR had a linear dynamic range from 10 to $10^8$ copies/reaction, with an efficiency of 94%. Total bacteria were enumerated using eubacterial 16S rRNA primers 1055f and 1392r, following standard procedures as described before.[31]

**Additive biokinetic model framework.** We calibrated and applied a previously described additive biokinetic model to interpret the experimental data.[20] The model is implemented in AQUASIM 2.1 and is available upon request from the authors. The model variables and rate expressions are summarized in **Table S1**. Briefly, the model considers a trace-level pollutant (carbofuran, $\boldsymbol{S_{TP}}$) and coincidental carbon substrates (AOC, $\boldsymbol{S_{AOC}}$) as potentially limiting growth substrates; all other growth substrates are considered to be in excess. The model also considers the trace-level pollutant degrader (strain KN65.2, $\boldsymbol{X_{KN65.2}}$) and the indigenous microbial community ($\boldsymbol{X_{BC}}$) as independent populations with independent growth dependencies. $\boldsymbol{X_{KN65.2}}$ grows on $\boldsymbol{S_{TP}}$ (with a yield of $\boldsymbol{Y_{TP,X}}$) and both $\boldsymbol{X_{KN65.2}}$ and $\boldsymbol{X_{BC}}$ grow on $\boldsymbol{S_{AOC}}$. Whereas $\boldsymbol{X_{BC}}$ can access the entire

pool of $S_{AOC}$ (i.e., the AOC is estimated based on the measured growth of $X_{BC}$),[17] only a fraction of the $S_{AOC}$ is available for $X_{KN65.2}$. Therefore, we divide the $S_{AOC}$ into two pools, $S_{AOC,X}$ and $S_{AOC,other}$, denoting the fraction simultaneously available to both $X_{KN65.2}$ and $X_{BC}$, and the fraction exclusively available to $X_{BC}$, respectively. Saturation-type substrate-dependencies (Monod) are assumed for all kinetic rate expressions. We assume growth on $S_{TP}$ and $S_{AOC}$ is additive, and that there are no direct interactions between the presence of $S_{AOC}$ and $X_{BC}$ on the growth of $X_{KN65.2}$ on $S_{TP}$. We also assume first order biomass decay.

**Estimation of model parameters.** We used data collected from experiments conducted according to scenarios (1) and (2) to parameterize the biokinetic model. We estimated growth and substrate utilization kinetic parameters ($\mu_{max}$ and $K_s$) for strain KN65.2 ($X_{KN65.2}$) and the indigenous microbial community ($X_{BC}$) on AOC by fitting the biokinetic model function to cell numbers by non-linear least-squares fitting. The standard deviation for parameter estimation was set to 10% to ensure the validity of the obtained parameter values.[20] The initial AOC concentrations available for $X_{KN65.2}$ and $X_{BC}$ in each water sample were estimated from the maximum measured cell concentrations from experimental scenarios (1) and (2) with previously reported yields on AOC:[12]

$$\text{AOC [mg L}^{-1}] = \frac{(\text{cells})\ \text{L}^{-1}}{1.0 \times 10^9\ \text{cells (mg AOC)}^{-1}} \quad (1)$$

Here, $1.0 \times 10^9$ cells (mg AOC)$^{-1}$ refers to the assumed cell yield $Y_{C/S}$.[12] The resulting model growth and substrate utilization kinetic parameters are summarized in **Table S2** alongside previously reported data on carbofuran utilization kinetics and resulting yield of strain KN65.2 in the absence of AOC.[10] A first order decay coefficient of 0.01 h$^{-1}$ was assumed, as it could not be estimated from the experiments because they did not continue sufficiently long into decay phase.

**Model simulations.** We used the parameterized kinetic model to simulate the biotransformation of carbofuran by strain KN65.2 in the presence of AOC and in the presence of AOC and the

indigenous microbial community. In the former simulation, we assumed only growth processes were relevant (P1 and P2 in **Table S1**) and compared the simulation results to the data from experimental scenario (3). In the latter simulation, we assumed all growth and decay processes were relevant (P1 through P6 in **Table S1**) and compared the simulation results to the data from experimental scenario (4). A summary describing the full model framework and the scenarios that were simulated is provided in **Figure S1**.

## RESULTS AND DISCUSSION

**Characterization of water samples.** We selected four water sources that had varying amounts and qualities of AOC and indigenous microbial communities of different environmental origin. The characterization of the GW, BF, SS, and SP water samples is given in **Table 1**. The pH of the water samples ranged between 7.6 and 8.1. Therefore, the neutral species of carbofuran was dominating in all experiments ($pK_a$=14.7). The specific conductivity of the water samples ranged between 290 and 676 µS $cm^{-1}$, which is a typical range for environmentally derived fresh water.[32]

The water samples differed significantly with regard to the amounts and types of organic carbon. The dissolved organic carbon concentrations (DOC) ranged over two orders of magnitude with GW having had the lowest (0.7 mg $L^{-1}$) and SP having had the highest concentration (10.0 mg $L^{-1}$). In addition, the fraction of labile organic carbon among the water samples may be quite different with even GW containing labile organic carbon derived from a variety of sources.[33, 34] We used SUVA to measure the degree of aromaticity of the DOC in each of the water samples as a surrogate for labile organic carbon or AOC quality (less aromaticity leads to more labile organic carbon).[35, 36] Waters with SUVA values >2 L mg $C^{-1}$ $m^{-1}$ (BF and SS) have relatively high fractions of hydrophobic, aromatic, and high molecular weight DOC, while waters with SUVA values <2 L mg $C^{-1}$ $m^{-1}$ (GW and SP) contain mostly hydrophilic, non-humic, and low molecular weight DOC

fractions.[37] Therefore, based on the SUVA measurements given in Table 1, GW and SP were expected to have the largest fractions of labile organic carbon.

As a more direct measure of AOC quality, we also estimated AOC in each of the water samples by measuring the growth of strain KN65.2 or the indigenous microbial community and assuming a yield of $10^9$ cells (mg AOC)$^{-1}$.[12] AOC can be considered as the fraction of DOC that is available for heterotrophic growth by the respective microbial populations and is a better measure of labile organic carbon than SUVA.[38] AOC consists of low molecular weight compounds derived from primary producers, of substances leaching from dying microorganisms, or of substances set free by enzymatic and (photo)chemical hydrolysis of more complex DOC.[13, 39] AOC values ($S_{AOC}$) of the water samples determined with the indigenous microbial community ranged between 0.40 mg L$^{-1}$ (BF) and 7.03 mg L$^{-1}$ (SP). Interestingly, AOC made up a larger percentage of the DOC for GW (66%), SP (70%), and SS (100%) than for BF (28%), confirming that SUVA is not a good estimator of labile organic carbon. The AOC values ($S_{AOC,X}$) for the water samples determined with strain KN65.2 were lower, but followed a similar trend in magnitude and percentage of DOC as determined for the indigenous microbial community. Importantly, the AOC value estimated for GW is lower than 0.01 mg L$^{-1}$, which is often considered a threshold value to support heterotrophic growth.[38]

**Estimation of kinetic parameters.** The kinetic parameters for the growth of the indigenous microbial community and strain KN65.2 on AOC were independently estimated from the experimental data for each water sample, as shown in **Figures S2** and **Figure 1A-D (circles)**, respectively. All of the cell density profiles could be adequately described assuming Monod growth kinetics, and the resulting kinetic parameters are given in **Table S2**. As was expected in fitting data of this type, independent estimation of $\mu_{max}$ and $K_s$ was challenging because those two

parameters are not separately identifiable.[40] Therefore, we constrained the estimation routine to only accept values for $K_s$ that were less than the initial AOC concentration for that water sample. Best fit curves (dotted lines) for growth of strain KN65.2 on the AOC present (circles) are shown in **Figure 1A-D**. Limited growth of strain KN65.2 was observed in GW and BF, whereas strain KN65.2 exceeded $10^8$ cells $L^{-1}$ in SS and approached $10^9$ cells $L^{-1}$ in SP. These differences are attributed to the quantity and quality of AOC and other nutrients present in the respective water samples and their availability for strain KN65.2.[34]

**Influence of AOC on growth of strain KN65.2 and carbofuran biotransformation.** Using the kinetic parameters estimated for strain KN65.2 from the data collected in experimental scenario (2), we simulated the expected growth of strain KN65.2 and the concomitant carbofuran biotransformation (i.e., utilization) in each of the water samples in the absence of the indigenous microbial community. We used the residual AOC estimated from each water sample as $\boldsymbol{S_{AOC,X}}$ and 1 mg $L^{-1}$ of carbofuran as $\boldsymbol{S_{TP}}$. The experimental data (squares) and the model simulation (solid line) for growth of strain KN65.2 and for the concomitant biotransformation of carbofuran are shown in **Figure 1A-H**.

The experimental results demonstrate that, in the presence of 1 mg $L^{-1}$ of carbofuran, the growth of strain KN65.2 is limited in GW and BF (**Figure 1A-B**). In fact, growth of strain KN65.2 in GW and BF was the same whether carbofuran had been provided as a supplement (squares) or not (circles). On the other hand, growth of strain KN65.2 exceeded $10^9$ cells $L^{-1}$ in SS and SP water when 1 mg $L^{-1}$ of carbofuran was added as a growth supplement. Strain KN65.2 achieved greater cell numbers with carbofuran as a supplement than with residual AOC alone (**Figure 1C-D**). We compared these data to those reported previously describing the growth of strain KN65.2 in AOC-restricted mineral media (including excess phosphorous and nitrogen nutrients) in the presence of

1 mg $L^{-1}$ of carbofuran as a supplement (**Figure 1C**, triangles).[10] The data from these previous experiments are the same in each panel and are provided as a reference for the experimental data reported here. We note that significantly more growth of strain KN65.2 was observed in our previous experiments in AOC-restricted mineral media when compared to the GW and BF samples reported here; though more growth was observed in SS and SP water here than in our previous experiments. This suggests that there might have been a limiting nutrient in the GW and BF water samples that specifically limited growth of strain KN65.2 (but not of the indigenous microbial community that was adapted to the oligotrophic conditions), even in the presence of a suitable growth substrate (carbofuran).[41] As a consequence, the simulations for strain KN65.2 growth in GW and BF (**Figure 1A-B**, squares) did not agree with the experimental data (**Figure 1A-B**, solid line) as the additive biokinetic model assumed that all other growth substrates were in excess. On the other hand, the simulations (**Figure 1C-D,** squares) in SS and SP agreed well with the experimental data (**Figure 1C-D**, solid line), providing some validation for the additive biokinetic model framework; the model simulations predict growth that is greater than the measured growth on either residual AOC or the supplemental carbofuran alone.

The experimental results also demonstrated that carbofuran was biotransformed in all water samples (**Figure 1E-H**). In GW and BF, the rate of carbofuran biotransformation was slower than predicted by our simulation, and in SS and SP the rate of carbofuran biotransformation agreed well with our predictions. It is interesting to note that we observed carbofuran biotransformation in GW and BF samples, but did not observe concomitant growth of strain KN65.2. It is also important to emphasize that the carbofuran biotransformation that we did observe occurred at a slower rate than one would have predicted based on carbofuran utilization kinetics and associated growth of strain KN65.2. These coupled observations provide strong evidence that the limited growth that was

observed for strain KN65.2 in GW and BF was not the result of growth-linked carbofuran utilization. While the low AOC and poor nutrient environment in GW and BF was expected to result in the expression of many accessory catabolic pathways,[11] it is not clear whether expression of the specific carbofuran catabolic pathway would have been favored under these conditions. The carbofuran biotransformation pathway is initiated with a carbamate hydrolysis that, by itself, is not expected to support growth and is known to be regulated differentially from subsequent biotransformation steps along the pathway to mineralization.[5] The biotransformation of carbofuran (but not mineralization) would then result in accumulation of metabolites that are not further metabolized. Our data, therefore, suggest that the carbofuran biotransformation observed in GW and BF did not lead to mineralization and, consequently, did not support growth of strain KN65.2. On the other hand, the good agreement between measured growth of strain KN65.2 and carbofuran biotransformation in SS and SP and our simulations suggests that strain KN65.2 grew on residual AOC as well as on carbofuran in these water samples, and that the carbofuran utilization kinetics can be adequately predicted when we treat this coupled growth as an additive biokinetic process. In conclusion, we note that the additive biokinetic model was able to simulate adequately the growth of strain KN65.2 and the concomitant biotransformation of carbofuran in natural waters in the presence of coincidental carbon substrates (i.e., AOC) when the environment also supports growth of strain KN65.2 in the absence of carbofuran. However, the additive biokinetic model does not adequately simulate the growth of strain KN65.2 and the concomitant biotransformation of carbofuran in natural waters that do not support growth or that suppress the catabolic pathway. This could have been the result of limiting growth nutrients for strain KN65.2 (but not the indigenous microbial community) in GW and BF or of repression of the catabolic pathway for carbofuran degradation under oligotrophic conditions.

**Influence of indigenous microbial community on growth of strain KN65.2 and carbofuran biotransformation.** Using the kinetic parameters estimated for the indigenous microbial community and strain KN65.2 from the data collected in experimental scenarios (1) and (2), respectively, we next simulated the expected growth of strain KN65.2 and the concomitant carbofuran biotransformation (i.e., utilization) in each of the water samples in the presence of the indigenous microbial community. We used the residual AOC that can be utilized by strain KN65.2 and the indigenous microbial community as $\boldsymbol{S_{AOC,X}}$, the residual AOC that can be utilized by the indigenous microbial community as $\boldsymbol{S_{AOC,other}}$, and 1 mg $L^{-1}$ of carbofuran as $\boldsymbol{S_{TP}}$. The experimental data (black squares) and the model simulation (solid line) for growth of the combined microbial community (strain KN65.2 + the indigenous microbial community) and the concomitant biotransformation of carbofuran are shown in **Figure 2A-H**. We also tracked the specific growth of strain KN65.2 by means of qPCR-based detection of the functional gene *cfdC*, encoding the putative carbofuran-phenol hydroxylase,[5] among total community DNA extracts (diamonds) and simulated the growth of strain KN65.2 using the kinetic parameters derived from experimental scenario (2) (dotted line).

The experimental results demonstrate that, in the presence of 1 mg $L^{-1}$ of carbofuran, growth of the combined microbial community (**Figure 2A-D,** filled squares) exceeded that which was observed when strain KN65.2 was present in the absence of the indigenous microbial community (**Figure 1A-D,** open squares). This was expected because the combined microbial community can access more of the residual AOC than strain KN65.2 can by itself. However, our simulations again predicted greater cell numbers for the combined microbial community in GW and BF than we observed experimentally (**Figure 2A-B**). Also, we observed more growth of strain KN65.2 in GW and BF experiments conducted in the presence of the indigenous microbial

community (diamonds) than we did in the absence of the indigenous microbial community (open squares). We attribute this latter finding to members of the indigenous microbial community breaking down AOC that was not previously accessible to strain KN65.2 into AOC that supported growth of strain KN65.2. Despite this added growth of strain KN65.2, our simulations of growth of strain KN65.2 in GW and BF predicted greater cell numbers than we observed experimentally. On the other hand, our simulations for the combined microbial community (solid line) agreed well with the experimental data (black squares) in SS and SP (**Figure 2C-D**), though we over predicted growth of strain KN65.2 (dotted line) in these simulations. Interestingly, strain KN65.2 grew less in experiments conducted in the presence of an indigenous microbial community (diamonds) than in the absence of an indigenous microbial community (open squares) in SS and SP. We attribute this finding to the indigenous microbial community utilizing a fraction of the residual AOC that supported growth of strain KN65.2 ($\boldsymbol{S_{AOC,X}}$), and perhaps also breakdown products of carbofuran generated by strain KN65.2, leaving less of the residual AOC or the AOC present in carbofuran to support growth of strain KN65.2. This interpretation would need to be confirmed by further experiments. In conclusion, the presence of an indigenous microbial community enhanced the growth of strain KN65.2 in low AOC or nutrient environments (GW and BF) and inhibited the growth of strain KN65.2 in high AOC or nutrient environments (SS and SP) likely due to competition effects.

The experimental results also demonstrate that carbofuran was biotransformed in all of the water samples, even in the presence of an indigenous microbial community (**Figure 2E-H**). In GW and BF, the rate of carbofuran biotransformation increased in the presence of an indigenous microbial community, in concordance with the increased cell density of strain KN65.2, though the rate of carbofuran biotransformation remained slower than predicted based on growth-linked

utilization (**Figure 2E-F *vs* Figure 1E-F**). This again suggests that the observed carbofuran biotransformation in GW and BF did not lead to mineralization, and may be restricted to the initial carbamate hydrolysis. Therefore, this implies that the rate of carbofuran biotransformation may have been enhanced in low AOC environments due to co-degradation between strain KN65.2 and the indigenous microbial community, though limiting factors may have still precluded expression of the full catabolic pathway. On the other hand, the presence of the indigenous microbial community had no effect on the rate of carbofuran removal for SS and SP and the experimental data agreed well with our simulations (**Figure 2G-H vs Figure 1G-H**), despite the observation that the indigenous microbial community limited the total growth of strain KN65.2 in terms of cell density. Our data, therefore, suggest that the presence of an indigenous microbial community had an overall benefit to carbofuran biotransformation by strain KN65.2 in each water sample type.

**Implications for biokinetic modeling of bio-augmentation systems.** It is essential to understand and describe the interactions of AOC and indigenous microbial communities on pesticide degradation in aquatic environments. An improved understanding of the interactions between AOC, indigenous microbial communities, and trace-level pesticide degraders will allow us to predict potential failure and success of bio-augmentation strategies for pesticide removal from aquatic systems that may include contaminated aquifers or biologically active sand filters used for drinking water production. In this research, we designed a series of experiments to explicitly challenge an additive biokinetic model to predict growth of degrader strains on trace-level pollutants and concomitant biotransformation of the pollutant. We found that under scenarios that support the growth of the degrader strain in the absence of a trace pollutant (water derived from a shallow stream (SS) and a stagnant pond (SP)), the degrader strain worked in cooperation with the indigenous microbial community and an additive biokinetic model could adequately predict

growth of the combined microbial community and the rate of pollutant utilization. However, under scenarios that did not support the growth of the degrader strain in the absence of a trace pollutant (water derived from groundwater (GW) and bank filtrate (BF)), growth of the degrader strain in the presence of the trace-level pollutant was limited and catabolic pathways may have been suppressed. These results support the utility of our additive biokinetic framework in some situations, and suggest that preliminary growth experiments can be useful for predicting the success of bio-augmentation. In future work, it will be important to identify the specific fractions of AOC or other trace nutrients that can stimulate the activity of bio-augmented strains in oligotrophic environments that otherwise do not support their growth.

## SUPPORTING INFORMATION

Supporting information is available that includes details of the model framework, details of the experimental matrix, and results of water characterization.

## ACKNOWLEDGEMENTS

This work was supported by the EU-FP7 project BIOTREAT (GA no.: 266039).

# FIGURE CAPTIONS

**Figure 1**. Results from batch experiments (discrete symbols) and model simulations (continuous lines) investigating (A-D) the growth of strain KN65.2 and (E-H) the biotransformation of carbofuran. We report the growth of KN65.2 only on residual AOC (circles; dotted lines) and on carbofuran in the presence of residual AOC (squares; solid line) in different water samples. The growth of KN65.2 on carbofuran in AOC-restricted mineral media (data from Helbling et al [10] in triangles and fitted with dot-dashed line) is shown in figure C. We report biotransformation of carbofuran in the presence of residual AOC for different water samples (E-H).

**Figure 2.** Results from batch experiments (discrete symbols) and model simulations (continuous lines) investigating (A-D) the growth of the combined microbial community (strain KN65.2 + indigenous microbial community) and the growth of strain KN65.2 and (E-H) the biotransformation of carbofuran. We report the combined microbial community on carbofuran in the presence of residual AOC (filled square; solid line), and KN65.2 on carbofuran in the presence of residual AOC and the indigenous microbial community (diamonds; dotted line) for different water samples. We report biotransformation of carbofuran in the presence of residual AOC and the indigenous microbial community for different water samples (E-H).

# TABLES

**TABLE 1.** Water quality characteristics of the water samples.

| | pH | Specific Conductivity [µS cm$^{-1}$] | DOC [mg L$^{-1}$] | [1]SUVA [L mg C$^{-1}$ m$^{-1}$] | [2]$S_{AOC}$ [mg L$^{-1}$] | [3]$S_{AOC,X}$ [mg L$^{-1}$] |
|---|---|---|---|---|---|---|
| **Ground water (GW)** | 7.8 | 490 | 0.70±0.02 | 1.4 | 0.46±0.11 | 0.008±0.001 |
| **Bank filtrate (BF)** | 7.6 | 676 | 1.3±0.01 | 2.6 | 0.37±0.08 | 0.021±0.005 |
| **Shallow stream (SS)** | 8.1 | 640 | 1.8±0.03 | 2.4 | 3.1±0.11 | 0.19±0.005 |
| **Stagnant pond (SP)** | 8.1 | 290 | 10.0±0.3 | 1.7 | 7.0±0.47 | 0.66±0.039 |

[1]SUVA = specific ultraviolet absorbance; [2]The assimilable organic carbon (AOC) utilized by the indigenous microbial community in each water sample; [3]The assimilable organic carbon (AOC) utilized by strain KN65.2 in each water sample.

## REFERENCES

(1) Benner, J.; Helbling, D. E.; Kohler, H. P. E.; Wittebol, J.; Kaiser, E.; Prasse, C.; Ternes, T. A.; Albers, C. N.; Aamand, J.; Horemans, B.; Springael, D.; Walravens, E.; Boon, N., Is biological treatment a viable alternative for micropollutant removal in drinking water treatment processes? *Water Res.* **2013,** *47*, (16), 5955-5976.

(2) Fenner, K.; Canonica, S.; Wackett, L. P.; Elsner, M., Evaluating pesticide degradation in the environment: blind spots and emerging opportunities. *Science* **2013,** *341*, (6147), 752-758.

(3) Moschet, C.; Wittmer, I.; Simovic, J.; Junghans, M.; Piazzoli, A.; Singer, H.; Stamm, C.; Leu, C.; Hollender, J., How a complete pesticide screening changes the assessment of surface water quality. *Environ. Sci. Technol.* **2014,** *48*, (10), 5423-5432.

(4) Sekhar, A.; Horemans, B.; Aamand, J.; Sorensen, S. R.; Vanhaecke, L.; Vanden Bussche, J.; Hofkens, J.; Springael, D., Surface colonization and activity of the 2,6-Dichlorobenzamide (BAM) degrading aminobacter sp strain MSH1 at macro- and micropollutant BAM concentrations. *Environ. Sci. Technol.* **2016,** *50*, (18), 10123-10133.

(5) Nguyen, T. P. O.; Helbling, D. E.; Bers, K.; Fida, T. T.; Wattiez, R.; Kohler, H. P. E.; Springael, D.; De Mot, R., Genetic and metabolic analysis of the carbofuran catabolic pathway in Novosphingobium sp KN65.2. *Appl. Microbiol. Biotechnol.* **2014,** *98*, (19), 8235-8252.

(6) Owsianiak, M.; Dechesne, A.; Binning, P. J.; Chambon, J. C.; Sorensen, S. R.; Smets, B. F., Evaluation of bioaugmentation with entrapped degrading cells as a soil remediation technology. *Environ. Sci. Technol.* **2010,** *44*, (19), 7622-7627.

(7) Scheutz, C.; Broholm, M. M.; Durant, N. D.; Weeth, E. B.; Jorgensen, T. H.; Dennis, P.; Jacobsen, C. S.; Cox, E. E.; Chambon, J. C.; Bjerg, P. L., Field evaluation of biological enhanced

reductive dechlorination of chloroethenes in clayey till. *Environ. Sci. Technol.* **2010,** *44*, (13), 5134-5141.

(8) Haig, S. J.; Gauchotte-Lindsay, C.; Collins, G.; Quince, C., Bioaugmentation mitigates the impact of estrogen on coliform-grazing protozoa in slow sand filters. *Environ. Sci. Technol.* **2016,** *50*, (6), 3101-3110.

(9) Albers, C. N.; Feld, L.; Ellegaard-Jensen, L.; Aamand, J., Degradation of trace concentrations of the persistent groundwater pollutant 2,6-dichlorobenzamide (BAM) in bioaugmented rapid sand filters. *Water Res.* **2015,** *83*, 61-70.

(10) Helbling, D. E.; Hammes, F.; Egli, T.; Kohler, H. P. E., Kinetics and yields of pesticide biodegradation at low substrate concentrations and under conditions restricting assimilable organic carbon. *Appl. Environ. Microbiol.* **2014,** *80*, (4), 1306-1313.

(11) Egli, T., How to live at very low substrate concentration. *Water Res.* **2010,** *44*, (17), 4826-4837.

(12) Hammes, F. A.; Egli, T., New method for assimilable organic carbon determination using flow-cytometric enumeration and a natural microbial consortium as inoculum. *Environ. Sci. Technol.* **2005,** *39*, (9), 3289-3294.

(13) Vital, M.; Hammes, F.; Egli, T., Escherichia coli O157 can grow in natural freshwater at low carbon concentrations. *Environ. Microbiol.* **2008,** *10*, (9), 2387-2396.

(14) Horemans, B.; Vandermaesen, J.; Breugelmans, P.; Hofkens, J.; Smolders, E.; Springael, D., The quantity and quality of dissolved organic matter as supplementary carbon source impacts the pesticide-degrading activity of a triple-species bacterial biofilm. *Appl. Microbiol. Biotechnol.* **2014,** *98*, (2), 931-943.

(15) Zhang, W. L.; Li, Y.; Wang, C.; Wang, P. F.; Hou, J.; Yu, Z. B.; Niu, L. H.; Wang, L. Q.; Wang, J., Modeling the Biodegradation of Bacterial Community Assembly Linked Antibiotics in River Sediment Using a Deterministic Stochastic Combined Model. *Environ. Sci. Technol.* **2016,** *50*, (16), 8788-8798.

(16) Song, D. J.; Kitamura, M.; Katayama, A., Approach for Estimating Microbial Growth and Biodegradation of Hydrocarbon Contaminants in Subsoil Based on Field Measurements: 2. Application in a Field Lysimeter Experiment. *Environ. Sci. Technol.* **2010,** *44*, (17), 6795-6801.

(17) Vital, M.; Hammes, F.; Egli, T., Competition of Escherichia coli O157 with a drinking water bacterial community at low nutrient concentrations. *Water Res.* **2012,** *46*, (19), 6279-6290.

(18) Van Nevel, S.; De Roy, K.; Boon, N., Bacterial invasion potential in water is determined by nutrient availability and the indigenous community. *FEMS Microbiol. Ecol.* **2013,** *85*, (3), 593-603.

(19) Horemans, B.; Breugelmans, P.; Saeys, W.; Springael, D., Soil-Bacterium Compatibility Model as a Decision-Making Tool for Soil Bioremediation. *Environ. Sci. Technol.* **2017,** *51*, (3), 1605-1615.

(20) Liu, L.; Helbling, D. E.; Kohler, H. P. E.; Smets, B. F., A model framework to describe growth-linked biodegradation of trace-level pollutants in the presence of coincidental carbon substrates and microbes. *Environ. Sci. Technol.* **2014,** *48*, (22), 13358-13366.

(21) Caldas, S. S.; Demoliner, A.; Costa, F. P.; D'Oca, M. G. M.; Primel, E. G., Pesticide residue determination in groundwater using solid-phase extraction and high-performance liquid chromatography with diode array detector and liquid chromatography-tandem mass spectrometry. *J. Braz. Chem. Soc* **2010,** *21*, (4), 642-650.

(22) Chiron, S.; Valverde, A.; FernandezAlba, A.; Barcelo, D., Automated sample preparation for monitoring groundwater pollution by carbamate insecticides and their transformation products. *J. AOAC Int.* **1995,** *78*, (6), 1346-1352.

(23) Chowdhury, M. A. Z.; Banik, S.; Uddin, B.; Moniruzzaman, M.; Karim, N.; Gan, S. H., Organophosphorus and carbamate pesticide residues detected in water samples collected from paddy and vegetable fields of the Savar and Dhamrai Upazilas in Bangladesh. *Int. J. Env. Res. Public Health* **2012,** *9*, (9), 3318-3329.

(24) De Llasera, M. P. G.; Bernal-Gonzalez, M., Presence of carbamate pesticides in environmental waters from the northwest of Mexico: Determination by liquid chromatography. *Water Res.* **2001,** *35*, (8), 1933-1940.

(25) Tariq, M. Y.; Afzal, S.; Hussain, I., Degradation and persistence of cotton pesticides in sandy loam soils from Punjab, Pakistan. *Environ. Res.* **2006,** *100*, (2), 184-196.

(26) Vryzas, Z.; Vassiliou, G.; Alexoudis, C.; Papadopoulou-Mourkidou, E., Spatial and temporal distribution of pesticide residues in surface waters in northeastern Greece. *Water Res.* **2009,** *43*, (1), 1-10.

(27) Helbling, D. E., Bioremediation of pesticide-contaminated water resources: the challenge of low concentrations. *Curr. Opin. Biotechnol.* **2015,** *33*, 142-148.

(28) Eaton, A. D.; Clesceri, L. S.; Franson, M. A. H.; Association, A. P. H.; Greenberg, A. E.; Rice, E. W.; Association, A. W. W.; Federation, W. E., *Standard methods for the examination of water & wastewater*. American Public Health Association: Washington, DC, 2005.

(29) Vital, M.; Füchslin, H. P.; Hammes, F.; Egli, T., Growth of Vibrio cholerae O1 Ogawa Eltor in freshwater. *Microbiology* **2007,** *153*, (7), 1993-2001.

(30) Hammes, F.; Berney, M.; Wang, Y. Y.; Vital, M.; Koster, O.; Egli, T., Flow-cytometric total bacterial cell counts as a descriptive microbiological parameter for drinking water treatment processes. *Water Res.* **2008,** *42*, (1-2), 269-277.

(31) Terada, A.; Lackner, S.; Kristensen, K.; Smets, B. F., Inoculum effects on community composition and nitritation performance of autotrophic nitrifying biofilm reactors with counter-diffusion geometry. *Environ. Microbiol.* **2010,** *12*, (10), 2858-2872.

(32) Walton, N. R. G., Electrical-conductivity and total dissolved solids - what is their precise relationship. *Desalination* **1989,** *72*, (3), 275-292.

(33) Arrieta, J. M.; Mayol, E.; Hansman, R. L.; Herndl, G. J.; Dittmar, T.; Duarte, C. M., Dilution limits dissolved organic carbon utilization in the deep ocean. *Science* **2015,** *348*, (6232), 331-333.

(34) Stegen, J. C.; Johnson, T.; Fredrickson, J. K.; Wilkins, M. J.; Konopka, A. E.; Nelson, W. C.; Arntzen, E. V.; Chrisler, W. B.; Chu, R. K.; Fansler, S. J.; Graham, E. B.; Kennedy, D. W.; Resch, C. T.; Tfaily, M.; Zachara, J., Influences of organic carbon speciation on hyporheic corridor biogeochemistry and microbial ecology. *Nat. Commun.* **2018,** *9*, 585.

(35) Weishaar, J. L.; Aiken, G. R.; Bergamaschi, B. A.; Fram, M. S.; Fujii, R.; Mopper, K., Evaluation of specific ultraviolet absorbance as an indicator of the chemical composition and reactivity of dissolved organic carbon. *Environ. Sci. Technol.* **2003,** *37*, (20), 4702-4708.

(36) Li, C. W.; Benjamin, M. M.; Korshin, G. V., Use of UV spectroscopy to characterize the reaction between NOM and free chlorine. *Environ. Sci. Technol.* **2000,** *34*, (12), 2570-2575.

(37) Ates, N.; Kitis, M.; Yetis, U., Formation of chlorination by-products. in waters with low SUVA-correlations with SUVA and differential UV spectroscopy. *Water Res.* **2007,** *41*, (18), 4139-4148.

528 (38) Escobar, I. C.; Randall, A. A.; Taylor, J. S., Bacterial growth in distribution systems: Effect
529 of assimilable organic carbon and biodegradable dissolved organic carbon. *Environ. Sci. Technol.*
530 **2001,** *35*, (17), 3442-3447.
531 (39) Rosenstock, B.; Zwisler, W.; Simon, M., Bacterial consumption of humic and non-humic low
532 and high molecular weight DOM and the effect of solar irradiation on the turnover of labile DOM
533 in the Southern Ocean. *Microb Ecol* **2005,** *50*, (1), 90-101.
534 (40) Simkins, S.; Mukherjee, R.; Alexander, M., 2 Approaches to modeling kinetics of
535 biodegradation by growing-cells and application of a 2-compartment model for mineralization
536 kinetics in sewage. *Appl. Environ. Microbiol.* **1986,** *51*, (6), 1153-1160.
537 (41) Singh, B. K.; Walker, A.; Morgan, J. A. W.; Wright, D. J., Biodegradation of chlorpyrifos by
538 Enterobacter strain B-14 and its use in bioremediation of contaminated soils. *Appl. Environ.*
539 *Microbiol.* **2004,** *70*, (8), 4855-4863.

540

# Modelling carbofuran biotransformation by *Novosphingobium* sp. KN65.2 in the presence of coincidental carbon and indigenous microbes

*Li Liu[1,2†], Damian E. Helbling[3,4*†], Hans-Peter E. Kohler[3], Barth F. Smets[1]**

[1]Department of Environmental Engineering, Technical, University of Denmark, Bygningstorvet 115, 2800 Kgs.Lyngby, Denmark;

[2]School of Chemistry, Beihang University, Beijing 100191, P. R. China;

[3]Eawag, Swiss Federal Institute of Aquatic Science and Technology, Department of Environmental Microbiology, Überlandstrasse 133, 8600 Dübendorf, Switzerland;

[4]School of Civil and Environmental Engineering, Cornell University, Ithaca, NY, USA.

***Corresponding authors:**

bfsm@env.dtu.dk, phone: +45 45 25 22 30, fax: +45 45 93 28 50

damian.helbling@cornell.edu, phone: +1 607 255 5146, fax: +1 607 255 9004

**†These authors contributed equally to this work**

20 **TOC Art**

21 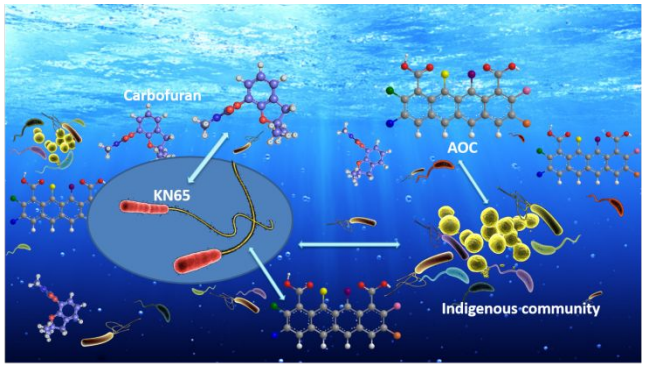

## ABSTRACT

The influence that coincidental carbon substrates (i.e., assimilable organic carbon, AOC) and indigenous microbial communities has on pesticide biotransformation by degrader strains in aquatic environments is poorly understood. We conducted batch experiments to investigate carbofuran biotransformation by *Novosphingobium* sp. KN65.2 using four environmentally derived water samples with varying amounts and types of AOC and indigenous microbial communities. We designed experimental scenarios to explore the influence of AOC and indigenous microbial communities on the growth of strain KN65.2 and the biotransformation of carbofuran. Relevant kinetic parameters were estimated from simpler experiments, and used to predict the growth of strain KN65.2 and the biotransformation of carbofuran in more complex experiments with an additive biokinetic model. We found that an additive biokinetic model adequately predicts the growth of strain KN65.2 and the rate of carbofuran biotransformation in natural waters that support the growth of strain KN65.2. However, our model over-predicts the growth of strain KN65.2 and the rate of carbofuran biotransformation in low-AOC environments. Overall, our results define the scope within which additive biokinetic models can be used to predict pesticide biotransformation in the presence of coincidental carbon substrates and indigenous microbial communities.

## INTRODUCTION

The presence of pesticides in aquatic systems, even at trace concentrations (ng-$\mu$g $L^{-1}$ range), might pose long-term environmental or human health risks.[1-3] Many pesticides are inherently biodegradable; one option to accelerate the removal of pesticides from contaminated water systems is through the addition of bacterial strains with metabolic capabilities to mineralize certain types of pesticides.[4, 5] This process is known as bio-augmentation,[6] and bio-augmentation might happen in a distributed (e.g., addition to aquifers) or localized (e.g., addition to unit processes in water treatment facilities) manner.[7, 8] The practice of bio-augmentation has, however, often failed or is only briefly successful.[9] One likely reason for this failure is that pesticide degrading strains are enriched and isolated at high pesticide concentrations and they cannot handle substrates at low concentrations.[10] In addition to the physiological challenges presented when growth substrates are present at trace concentrations,[11] there are at least two other fundamental considerations that have rarely been explored when evaluating pesticide bio-augmentation scenarios. First, natural water systems contain assimilable organic carbon (AOC) consisting of a complex mixture of substrates in addition to trace-levels of pesticides.[12, 13] The presence of AOC, which we refer to as coincidental carbon substrates, supports the growth of indigenous microbial communities and may or may not support the growth of the added pesticide degrader. It is also unclear whether the presence of AOC, typically at higher concentrations than the pesticide in question, would result in physiological changes in pesticide degraders and could lead to the down regulation of relevant pesticide catabolic pathways.[14-16] Second, natural waters contain indigenous microbial communities, and their presence can be a key factor for pesticide biodegradation. For example, indigenous microbial communities might compete for AOC or other essential nutrients and affect the density and fate of the pesticide degraders.[17, 18]

To the best of our knowledge, the literature lacks reports on growth measurements of specific pesticide degraders with concomitant measurements of pesticide biodegradation at low concentrations *in the presence* of AOC and indigenous microbial communities. We believe it is essential to understand and describe, using suitable models, the interactions between AOC and indigenous microbial communities and pesticide degradation in aquatic environments. Such knowledge would allow us to predict potential failure and success of bio-augmentation strategies for pesticide removal from aquatic systems. Complementary approaches, based on partial least square analysis, have been examined to predict strain survival and biodegradation activity in contaminated soils based on soil physico-chemical soil characteristics.[19] In this work, we studied the removal of the carbamate insecticide carbofuran by *Novosphingobium* sp. KN65.2, a strain that can mineralize carbofuran as the sole carbon source[5] in batch experiments with increasing complexity. We conducted the experiments using water derived from a variety of natural sources that contained varying amounts and types of AOC. Experiments were conducted to explicitly measure growth of strain KN65.2 on AOC in the absence of an indigenous microbial community, growth of the indigenous microbial community on AOC in the absence of strain KN65.2, growth of strain KN65.2 on AOC and carbofuran in the absence of an indigenous microbial community, and growth of both the indigenous microbial community and strain KN65.2 on AOC and carbofuran. In the latter two cases, we also measured carbofuran biotransformation. In previous work, we measured growth and carbofuran utilization kinetics of KN65.2 in the absence of AOC.[10] We also previously introduced an additive biokinetic model framework to describe growth-linked biodegradation of trace-level pollutants in the presence of coincidental carbon substrates and indigenous microbial communities, which we tentatively validated against limited literature-reported experimental data.[20] The dataset generated by the experiments reported here allows for a

more thorough evaluation of the proposed biokinetic model, which facilitates a full interpretation of the experimental results and leads to generalizable insights on the fundamentals of trace-level pesticide degradation in natural systems.

## MATERIALS AND METHODS

**Carbofuran and strain KN65.2.** We selected carbofuran as the model pesticide because it is frequently measured in surface and groundwater resources[21-26] and its occurrence in drinking water is regulated around the world.[27] We purchased carbofuran (99.9% purity) from Sigma-Aldrich (Seelze, Germany) and prepared spike solutions in AOC-restricted mineral medium at 100 mg $L^{-1}$ as previously described.[10] *Novosphingobium* sp. strain KN65.2 has the ability to mineralize carbofuran, and the biotransformation pathway is initiated by carbamate hydrolysis.[5] We received strain KN65.2 as a streak on an R2A agar plate from D. Springael *(Department of Earth and Environmental Sciences, KU Leuven).* A single colony was picked from the agar plate and added to 5 mL of sterilized LB medium. Cells were grown to early-stationary phase and diluted to approximately 15 % glycerol (0.5 mL of 50 % sterile glycerol added to 1 mL cell culture) and stored at -80 °C.

**Environmental water samples.** We collected water from four sources: groundwater (GW); bank filtrate (BF); shallow stream (SS); and stagnant pond (SP) near Dübendorf (CH). We reasoned that each of the water samples would contain varying quantities and qualities of AOC and diverse indigenous microbial communities. The samples were collected in 2 L trace clean glass bottles and pasteurized (30 min at 60°C) within 30 minutes of sampling as previously described.[10] A sufficient volume of each sample was preserved without pasteurization to allow for subsequent re-inoculation of the indigenous microbial community. All water samples were characterized for

dissolved organic carbon (DOC), specific UV absorbance (SUVA), pH, and specific conductivity following standard procedures.[28]

**Batch Experiments.** All glassware and caps used for batch experiments were treated rigorously to remove any residual AOC as previously described.[17, 29] Aliquots of 20 mL of the pasteurized water samples were filtered through a 0.1 μm Millex® syringe filter (Millipore, Billerica, MA, USA) into a 40 mL borosilicate glass vial. The 0.1 μm Millex® syringe filter was selected to ensure that all microorganisms were removed and to limit the leaching of AOC from the filters into the samples; the small pore size may have removed a negligible amount of larger AOC constituents. The borosilicate glass vials were again pasteurized (30 min at 60°C) to ensure sterile conditions. We designed four experimental scenarios to meet the project objectives (See Fig 1 in [20]). *First*, the indigenous microbial community was re-introduced into three vials at a concentration of $10^3$ cells $mL^{-1}$ and growth on the residual AOC was measured by flow cytometry. The inoculum was derived from unpasteurized water samples and cells in the inoculum were quantified by means of flow cytometry. *Second*, strain KN65.2 was spiked into three vials at a concentration of $10^3$ cells $mL^{-1}$ and growth on the residual AOC was measured by flow cytometry. The inoculum was prepared from the frozen glycerol stock and grown in mineral medium amended with approximately 10 mg $L^{-1}$ of carbofuran as previously described;[10] cells were washed in mineral medium three times to remove any residual AOC prior to inoculation in experiments. *Third*, strain KN65.2 was spiked into three vials at a concentration of $10^3$ cells $mL^{-1}$ along with 1 mg $L^{-1}$ of carbofuran. Growth of strain KN65.2 on residual AOC plus carbofuran was measured by flow cytometry and carbofuran biotransformation was measured by HPLC-UV. *Fourth*, the indigenous microbial community and strain KN65.2 were both added to three vials at a concentration of $10^3$ cells $mL^{-1}$ along with 1 mg $L^{-1}$ of carbofuran. Growth of the combined microbial community on

residual AOC and carbofuran was measured by flow cytometry, growth of strain KN65.2 was inferred from qPCR-based detection of KN65.2 in total community DNA extracts, and carbofuran biotransformation was measured by HPLC-UV. All batch experiments were conducted at 30 °C. Samples were taken at the time of inoculation and periodically thereafter until cell density measurements suggested stationary phase or carbofuran concentration was below the limit of detection (<0.05 mg $L^{-1}$).

**Quantification of growth by flow cytometry.** Cell densities were measured on a BD Accuri C6 Flow Cytometer (Erembodegem, Belgium). Aliquots of 500 µL from a batch experiment were combined with 5 µL of SYBR Green stain (Molecular Probes, Ba 154 sel, Switzerland) diluted 100-fold in dimethylsulfoxide (Fluka Chemie AG, Buchs, Switzerland) in a 1.5 mL plastic centrifuge tube (Greiner Bio One, Frickenhausen, Germany), vortexed briefly, and incubated in the dark at 40 ºC for 10 minutes. For cell densities less than $5 \times 10^5$ cells $mL^{-1}$, samples were measured directly on the BD Accuri C6 Flow Cytometer without dilution; for cell densities greater than $5 \times 10^5$ cells $mL^{-1}$, samples were diluted in filter-sterilized water. Data were analyzed with the CFlow v1.0.227.4 flow cytometry software. Enumeration was achieved with signals collected on the gated combined 533 nm/670nm density plot as previously described.[30]

**Quantification of carbofuran biotransformation.** HPLC-UV analyses were performed on a Gynkotek system with a Dionex ASI-100 autosampler and a UVD 340U diode array detector. Carbofuran was separated on a Nucleosil 100-5 C18 HD column (250×4.0 mm) with an octadecyl modified high density silica stationary phase (Macherey-Nagel, Düren, Germany). The HPLC was operated isocratically at a flow rate of 0.7 mL $min^{-1}$ with 55 % methanol and 45 % nanopure water eluents. Limits of quantification for carbofuran were less than 0.05 mg $L^{-1}$ with a 50 µL injection volume. The Chromeleon Client v6.6 (Dionex) was used for chromatogram analysis.

**Quantification of growth of strain KN65.2 by means of qPCR.** The collected cells were subject to DNA extraction using the MP FastDNA™ SPIN Kit (MP Biomedicals LLC., Solon, USA) following manufacturer's instructions. Concentration and purity of extracted DNA were checked by spectrophotometry (NanoDrop Technologies, Wilmington, DE, USA). qPCR was carried out on extracted DNA samples to determine the relative abundance of KN65.2 cells based on the *cfdC* gene and the 16S rRNA gene as targets for quantification of KN65.2 and all bacteria, respectively. For *cfdC* detection, primers $cfdC_{for}$: CCGCTCATGCCGTTTATCTAC and $cfdC_{rev}$: GGTTTCCAGATCGAACTCGC, were used with a PCR program consisting of an initial 5 min. denaturation at 94°C, 35 cycles of (94°C: 30 s; 54°C: 20 s; 72°C: 30 s) and final 5 min at 72°C. A unique product size was 252 bp, with melting at 87-88 °C. An *E. coli* clone carrying a *BamHI* fragment of the *cfdC* gene served as source for calibration curves. The *cfdC* qPCR had a linear dynamic range from 10 to $10^8$ copies/reaction, with an efficiency of 94%. Total bacteria were enumerated using eubacterial 16S rRNA primers 1055f and 1392r, following standard procedures as described before.[31]

**Additive biokinetic model framework.** We calibrated and applied a previously described additive biokinetic model to interpret the experimental data.[20] The model is implemented in AQUASIM 2.1 and is available upon request from the authors. The model variables and rate expressions are summarized in **Table S1**. Briefly, the model considers a trace-level pollutant (carbofuran, $\boldsymbol{S_{TP}}$) and coincidental carbon substrates (AOC, $\boldsymbol{S_{AOC}}$) as potentially limiting growth substrates; all other growth substrates are considered to be in excess. The model also considers the trace-level pollutant degrader (strain KN65.2, $\boldsymbol{X_{KN65.2}}$) and the indigenous microbial community ($\boldsymbol{X_{BC}}$) as independent populations with independent growth dependencies. $\boldsymbol{X_{KN65.2}}$ grows on $\boldsymbol{S_{TP}}$ (with a yield of $\boldsymbol{Y_{TP,X}}$) and both $\boldsymbol{X_{KN65.2}}$ and $\boldsymbol{X_{BC}}$ grow on $\boldsymbol{S_{AOC}}$. Whereas $\boldsymbol{X_{BC}}$ can access the entire

pool of $S_{AOC}$ (i.e., the AOC is estimated based on the measured growth of $X_{BC}$),[17] only a fraction of the $S_{AOC}$ is available for $X_{KN65.2}$. Therefore, we divide the $S_{AOC}$ into two pools, $S_{AOC,X}$ and $S_{AOC,other}$, denoting the fraction simultaneously available to both $X_{KN65.2}$ and $X_{BC}$, and the fraction exclusively available to $X_{BC}$, respectively. Saturation-type substrate-dependencies (Monod) are assumed for all kinetic rate expressions. We assume growth on $S_{TP}$ and $S_{AOC}$ is additive, and that there are no direct interactions between the presence of $S_{AOC}$ and $X_{BC}$ on the growth of $X_{KN65.2}$ on $S_{TP}$. We also assume first order biomass decay.

**Estimation of model parameters.** We used data collected from experiments conducted according to scenarios (1) and (2) to parameterize the biokinetic model. We estimated growth and substrate utilization kinetic parameters ($\mu_{max}$ and $K_s$) for strain KN65.2 ($X_{KN65.2}$) and the indigenous microbial community ($X_{BC}$) on AOC by fitting the biokinetic model function to cell numbers by non-linear least-squares fitting. The standard deviation for parameter estimation was set to 10% to ensure the validity of the obtained parameter values.[20] The initial AOC concentrations available for $X_{KN65.2}$ and $X_{BC}$ in each water sample were estimated from the maximum measured cell concentrations from experimental scenarios (1) and (2) with previously reported yields on AOC:[12]

$$\text{AOC [mg L}^{-1}] = \frac{(\text{cells})\ \text{L}^{-1}}{1.0 \times 10^9\ \text{cells (mg AOC)}^{-1}} \quad (1)$$

Here, $1.0 \times 10^9$ cells (mg AOC)$^{-1}$ refers to the assumed cell yield $Y_{C/S}$.[12] The resulting model growth and substrate utilization kinetic parameters are summarized in **Table S2** alongside previously reported data on carbofuran utilization kinetics and resulting yield of strain KN65.2 in the absence of AOC.[10] A first order decay coefficient of 0.01 h$^{-1}$ was assumed, as it could not be estimated from the experiments because they did not continue sufficiently long into decay phase.

**Model simulations.** We used the parameterized kinetic model to simulate the biotransformation of carbofuran by strain KN65.2 in the presence of AOC and in the presence of AOC and the

199 indigenous microbial community. In the former simulation, we assumed only growth processes
200 were relevant (P1 and P2 in **Table S1**) and compared the simulation results to the data from
201 experimental scenario (3). In the latter simulation, we assumed all growth and decay processes
202 were relevant (P1 through P6 in **Table S1**) and compared the simulation results to the data from
203 experimental scenario (4). A summary describing the full model framework and the scenarios that
204 were simulated is provided in **Figure S1**.

205 ## RESULTS AND DISCUSSION

206 **Characterization of water samples.** We selected four water sources that had varying amounts
207 and qualities of AOC and indigenous microbial communities of different environmental origin.
208 The characterization of the GW, BF, SS, and SP water samples is given in **Table 1**. The pH of the
209 water samples ranged between 7.6 and 8.1. Therefore, the neutral species of carbofuran was
210 dominating in all experiments ($pK_a$=14.7). The specific conductivity of the water samples ranged
211 between 290 and 676 µS $cm^{-1}$, which is a typical range for environmentally derived fresh water.[32]

212 The water samples differed significantly with regard to the amounts and types of organic
213 carbon. The dissolved organic carbon concentrations (DOC) ranged over two orders of magnitude
214 with GW having had the lowest (0.7 mg $L^{-1}$) and SP having had the highest concentration (10.0
215 mg $L^{-1}$). In addition, the fraction of labile organic carbon among the water samples may be quite
216 different with even GW containing labile organic carbon derived from a variety of sources.[33, 34]
217 We used SUVA to measure the degree of aromaticity of the DOC in each of the water samples as
218 a surrogate for labile organic carbon or AOC quality (less aromaticity leads to more labile organic
219 carbon).[35, 36] Waters with SUVA values >2 L mg $C^{-1}$ $m^{-1}$ (BF and SS) have relatively high fractions
220 of hydrophobic, aromatic, and high molecular weight DOC, while waters with SUVA values <2 L
221 mg $C^{-1}$ $m^{-1}$ (GW and SP) contain mostly hydrophilic, non-humic, and low molecular weight DOC

fractions.[37] Therefore, based on the SUVA measurements given in Table 1, GW and SP were expected to have the largest fractions of labile organic carbon.

As a more direct measure of AOC quality, we also estimated AOC in each of the water samples by measuring the growth of strain KN65.2 or the indigenous microbial community and assuming a yield of $10^9$ cells (mg AOC)$^{-1}$.[12] AOC can be considered as the fraction of DOC that is available for heterotrophic growth by the respective microbial populations and is a better measure of labile organic carbon than SUVA.[38] AOC consists of low molecular weight compounds derived from primary producers, of substances leaching from dying microorganisms, or of substances set free by enzymatic and (photo)chemical hydrolysis of more complex DOC.[13, 39] AOC values ($\boldsymbol{S_{AOC}}$) of the water samples determined with the indigenous microbial community ranged between 0.40 mg L$^{-1}$ (BF) and 7.03 mg L$^{-1}$ (SP). Interestingly, AOC made up a larger percentage of the DOC for GW (66%), SP (70%), and SS (100%) than for BF (28%), confirming that SUVA is not a good estimator of labile organic carbon. The AOC values ($\boldsymbol{S_{AOC,X}}$) for the water samples determined with strain KN65.2 were lower, but followed a similar trend in magnitude and percentage of DOC as determined for the indigenous microbial community. Importantly, the AOC value estimated for GW is lower than 0.01 mg L$^{-1}$, which is often considered a threshold value to support heterotrophic growth.[38]

**Estimation of kinetic parameters.** The kinetic parameters for the growth of the indigenous microbial community and strain KN65.2 on AOC were independently estimated from the experimental data for each water sample, as shown in **Figures S2** and **Figure 1A-D (circles),** respectively. All of the cell density profiles could be adequately described assuming Monod growth kinetics, and the resulting kinetic parameters are given in **Table S2**. As was expected in fitting data of this type, independent estimation of $\mu_{max}$ and $K_s$ was challenging because those two

parameters are not separately identifiable.[40] Therefore, we constrained the estimation routine to only accept values for $K_s$ that were less than the initial AOC concentration for that water sample. Best fit curves (dotted lines) for growth of strain KN65.2 on the AOC present (circles) are shown in **Figure 1A-D**. Limited growth of strain KN65.2 was observed in GW and BF, whereas strain KN65.2 exceeded $10^8$ cells $L^{-1}$ in SS and approached $10^9$ cells $L^{-1}$ in SP. These differences are attributed to the quantity and quality of AOC and other nutrients present in the respective water samples and their availability for strain KN65.2.[34]

**Influence of AOC on growth of strain KN65.2 and carbofuran biotransformation.** Using the kinetic parameters estimated for strain KN65.2 from the data collected in experimental scenario (2), we simulated the expected growth of strain KN65.2 and the concomitant carbofuran biotransformation (i.e., utilization) in each of the water samples in the absence of the indigenous microbial community. We used the residual AOC estimated from each water sample as $\boldsymbol{S_{AOC,X}}$ and 1 mg $L^{-1}$ of carbofuran as $\boldsymbol{S_{TP}}$. The experimental data (squares) and the model simulation (solid line) for growth of strain KN65.2 and for the concomitant biotransformation of carbofuran are shown in **Figure 1A-H**.

The experimental results demonstrate that, in the presence of 1 mg $L^{-1}$ of carbofuran, the growth of strain KN65.2 is limited in GW and BF (**Figure 1A-B**). In fact, growth of strain KN65.2 in GW and BF was the same whether carbofuran had been provided as a supplement (squares) or not (circles). On the other hand, growth of strain KN65.2 exceeded $10^9$ cells $L^{-1}$ in SS and SP water when 1 mg $L^{-1}$ of carbofuran was added as a growth supplement. Strain KN65.2 achieved greater cell numbers with carbofuran as a supplement than with residual AOC alone (**Figure 1C-D**). We compared these data to those reported previously describing the growth of strain KN65.2 in AOC-restricted mineral media (including excess phosphorous and nitrogen nutrients) in the presence of

1 mg $L^{-1}$ of carbofuran as a supplement (**Figure 1C**, triangles).[10] The data from these previous experiments are the same in each panel and are provided as a reference for the experimental data reported here. We note that significantly more growth of strain KN65.2 was observed in our previous experiments in AOC-restricted mineral media when compared to the GW and BF samples reported here; though more growth was observed in SS and SP water here than in our previous experiments. This suggests that there might have been a limiting nutrient in the GW and BF water samples that specifically limited growth of strain KN65.2 (but not of the indigenous microbial community that was adapted to the oligotrophic conditions), even in the presence of a suitable growth substrate (carbofuran).[41] As a consequence, the simulations for strain KN65.2 growth in GW and BF (**Figure 1A-B**, squares) did not agree with the experimental data (**Figure 1A-B**, solid line) as the additive biokinetic model assumed that all other growth substrates were in excess. On the other hand, the simulations (**Figure 1C-D,** squares) in SS and SP agreed well with the experimental data (**Figure 1C-D**, solid line), providing some validation for the additive biokinetic model framework; the model simulations predict growth that is greater than the measured growth on either residual AOC or the supplemental carbofuran alone.

The experimental results also demonstrated that carbofuran was biotransformed in all water samples (**Figure 1E-H**). In GW and BF, the rate of carbofuran biotransformation was slower than predicted by our simulation, and in SS and SP the rate of carbofuran biotransformation agreed well with our predictions. It is interesting to note that we observed carbofuran biotransformation in GW and BF samples, but did not observe concomitant growth of strain KN65.2. It is also important to emphasize that the carbofuran biotransformation that we did observe occurred at a slower rate than one would have predicted based on carbofuran utilization kinetics and associated growth of strain KN65.2. These coupled observations provide strong evidence that the limited growth that was

observed for strain KN65.2 in GW and BF was not the result of growth-linked carbofuran utilization. While the low AOC and poor nutrient environment in GW and BF was expected to result in the expression of many accessory catabolic pathways,[11] it is not clear whether expression of the specific carbofuran catabolic pathway would have been favored under these conditions. The carbofuran biotransformation pathway is initiated with a carbamate hydrolysis that, by itself, is not expected to support growth and is known to be regulated differentially from subsequent biotransformation steps along the pathway to mineralization.[5] The biotransformation of carbofuran (but not mineralization) would then result in accumulation of metabolites that are not further metabolized. Our data, therefore, suggest that the carbofuran biotransformation observed in GW and BF did not lead to mineralization and, consequently, did not support growth of strain KN65.2. On the other hand, the good agreement between measured growth of strain KN65.2 and carbofuran biotransformation in SS and SP and our simulations suggests that strain KN65.2 grew on residual AOC as well as on carbofuran in these water samples, and that the carbofuran utilization kinetics can be adequately predicted when we treat this coupled growth as an additive biokinetic process. In conclusion, we note that the additive biokinetic model was able to simulate adequately the growth of strain KN65.2 and the concomitant biotransformation of carbofuran in natural waters in the presence of coincidental carbon substrates (i.e., AOC) when the environment also supports growth of strain KN65.2 in the absence of carbofuran. However, the additive biokinetic model does not adequately simulate the growth of strain KN65.2 and the concomitant biotransformation of carbofuran in natural waters that do not support growth or that suppress the catabolic pathway. This could have been the result of limiting growth nutrients for strain KN65.2 (but not the indigenous microbial community) in GW and BF or of repression of the catabolic pathway for carbofuran degradation under oligotrophic conditions.

**Influence of indigenous microbial community on growth of strain KN65.2 and carbofuran biotransformation.** Using the kinetic parameters estimated for the indigenous microbial community and strain KN65.2 from the data collected in experimental scenarios (1) and (2), respectively, we next simulated the expected growth of strain KN65.2 and the concomitant carbofuran biotransformation (i.e., utilization) in each of the water samples in the presence of the indigenous microbial community. We used the residual AOC that can be utilized by strain KN65.2 and the indigenous microbial community as $\boldsymbol{S}_{\mathbf{AOC,X}}$, the residual AOC that can be utilized by the indigenous microbial community as $\boldsymbol{S}_{\mathbf{AOC,other}}$, and 1 mg $L^{-1}$ of carbofuran as $\boldsymbol{S}_{\mathbf{TP}}$. The experimental data (black squares) and the model simulation (solid line) for growth of the combined microbial community (strain KN65.2 + the indigenous microbial community) and the concomitant biotransformation of carbofuran are shown in **Figure 2A-H**. We also tracked the specific growth of strain KN65.2 by means of qPCR-based detection of the functional gene *cfdC*, encoding the putative carbofuran-phenol hydroxylase,[5] among total community DNA extracts (diamonds) and simulated the growth of strain KN65.2 using the kinetic parameters derived from experimental scenario (2) (dotted line).

The experimental results demonstrate that, in the presence of 1 mg $L^{-1}$ of carbofuran, growth of the combined microbial community (**Figure 2A-D,** filled squares) exceeded that which was observed when strain KN65.2 was present in the absence of the indigenous microbial community (**Figure 1A-D,** open squares). This was expected because the combined microbial community can access more of the residual AOC than strain KN65.2 can by itself. However, our simulations again predicted greater cell numbers for the combined microbial community in GW and BF than we observed experimentally (**Figure 2A-B**). Also, we observed more growth of strain KN65.2 in GW and BF experiments conducted in the presence of the indigenous microbial

community (diamonds) than we did in the absence of the indigenous microbial community (open squares). We attribute this latter finding to members of the indigenous microbial community breaking down AOC that was not previously accessible to strain KN65.2 into AOC that supported growth of strain KN65.2. Despite this added growth of strain KN65.2, our simulations of growth of strain KN65.2 in GW and BF predicted greater cell numbers than we observed experimentally. On the other hand, our simulations for the combined microbial community (solid line) agreed well with the experimental data (black squares) in SS and SP (**Figure 2C-D**), though we over predicted growth of strain KN65.2 (dotted line) in these simulations. Interestingly, strain KN65.2 grew less in experiments conducted in the presence of an indigenous microbial community (diamonds) than in the absence of an indigenous microbial community (open squares) in SS and SP. We attribute this finding to the indigenous microbial community utilizing a fraction of the residual AOC that supported growth of strain KN65.2 ($\boldsymbol{S_{AOC,X}}$), and perhaps also breakdown products of carbofuran generated by strain KN65.2, leaving less of the residual AOC or the AOC present in carbofuran to support growth of strain KN65.2. This interpretation would need to be confirmed by further experiments. In conclusion, the presence of an indigenous microbial community enhanced the growth of strain KN65.2 in low AOC or nutrient environments (GW and BF) and inhibited the growth of strain KN65.2 in high AOC or nutrient environments (SS and SP) likely due to competition effects.

The experimental results also demonstrate that carbofuran was biotransformed in all of the water samples, even in the presence of an indigenous microbial community (**Figure 2E-H**). In GW and BF, the rate of carbofuran biotransformation increased in the presence of an indigenous microbial community, in concordance with the increased cell density of strain KN65.2, though the rate of carbofuran biotransformation remained slower than predicted based on growth-linked

utilization (**Figure 2E-F *vs* Figure 1E-F**). This again suggests that the observed carbofuran biotransformation in GW and BF did not lead to mineralization, and may be restricted to the initial carbamate hydrolysis. Therefore, this implies that the rate of carbofuran biotransformation may have been enhanced in low AOC environments due to co-degradation between strain KN65.2 and the indigenous microbial community, though limiting factors may have still precluded expression of the full catabolic pathway. On the other hand, the presence of the indigenous microbial community had no effect on the rate of carbofuran removal for SS and SP and the experimental data agreed well with our simulations (**Figure 2G-H vs Figure 1G-H**), despite the observation that the indigenous microbial community limited the total growth of strain KN65.2 in terms of cell density. Our data, therefore, suggest that the presence of an indigenous microbial community had an overall benefit to carbofuran biotransformation by strain KN65.2 in each water sample type.

**Implications for biokinetic modeling of bio-augmentation systems.** It is essential to understand and describe the interactions of AOC and indigenous microbial communities on pesticide degradation in aquatic environments. An improved understanding of the interactions between AOC, indigenous microbial communities, and trace-level pesticide degraders will allow us to predict potential failure and success of bio-augmentation strategies for pesticide removal from aquatic systems that may include contaminated aquifers or biologically active sand filters used for drinking water production. In this research, we designed a series of experiments to explicitly challenge an additive biokinetic model to predict growth of degrader strains on trace-level pollutants and concomitant biotransformation of the pollutant. We found that under scenarios that support the growth of the degrader strain in the absence of a trace pollutant (water derived from a shallow stream (SS) and a stagnant pond (SP)), the degrader strain worked in cooperation with the indigenous microbial community and an additive biokinetic model could adequately predict

383 growth of the combined microbial community and the rate of pollutant utilization. However, under
384 scenarios that did not support the growth of the degrader strain in the absence of a trace pollutant
385 (water derived from groundwater (GW) and bank filtrate (BF)), growth of the degrader strain in
386 the presence of the trace-level pollutant was limited and catabolic pathways may have been
387 suppressed. These results support the utility of our additive biokinetic framework in some
388 situations, and suggest that preliminary growth experiments can be useful for predicting the
389 success of bio-augmentation. In future work, it will be important to identify the specific fractions
390 of AOC or other trace nutrients that can stimulate the activity of bio-augmented strains in
391 oligotrophic environments that otherwise do not support their growth.

392 ## SUPPORTING INFORMATION

393 Supporting information is available that includes details of the model framework, details of the
394 experimental matrix, and results of water characterization.

395 ## ACKNOWLEDGEMENTS

396 This work was supported by the EU-FP7 project BIOTREAT (GA no.: 266039).

## FIGURE CAPTIONS

**Figure 1**. Results from batch experiments (discrete symbols) and model simulations (continuous lines) investigating (A-D) the growth of strain KN65.2 and (E-H) the biotransformation of carbofuran. We report the growth of KN65.2 only on residual AOC (circles; dotted lines) and on carbofuran in the presence of residual AOC (squares; solid line) in different water samples. The growth of KN65.2 on carbofuran in AOC-restricted mineral media (data from Helbling et al [10] in triangles and fitted with dot-dashed line) is shown in figure C. We report biotransformation of carbofuran in the presence of residual AOC for different water samples (E-H).

**Figure 2.** Results from batch experiments (discrete symbols) and model simulations (continuous lines) investigating (A-D) the growth of the combined microbial community (strain KN65.2 + indigenous microbial community) and the growth of strain KN65.2 and (E-H) the biotransformation of carbofuran. We report the combined microbial community on carbofuran in the presence of residual AOC (filled square; solid line), and KN65.2 on carbofuran in the presence of residual AOC and the indigenous microbial community (diamonds; dotted line) for different water samples. We report biotransformation of carbofuran in the presence of residual AOC and the indigenous microbial community for different water samples (E-H).

# TABLES

**TABLE 1.** Water quality characteristics of the water samples.

| | pH | Specific Conductivity [µS cm$^{-1}$] | DOC [mg L$^{-1}$] | [1]SUVA [L mg C$^{-1}$ m$^{-1}$] | [2]$S_{AOC}$ [mg L$^{-1}$] | [3]$S_{AOC,X}$ [mg L$^{-1}$] |
|---|---|---|---|---|---|---|
| **Ground water (GW)** | 7.8 | 490 | 0.70±0.02 | 1.4 | 0.46±0.11 | 0.008±0.001 |
| **Bank filtrate (BF)** | 7.6 | 676 | 1.3±0.01 | 2.6 | 0.37±0.08 | 0.021±0.005 |
| **Shallow stream (SS)** | 8.1 | 640 | 1.8±0.03 | 2.4 | 3.1±0.11 | 0.19±0.005 |
| **Stagnant pond (SP)** | 8.1 | 290 | 10.0±0.3 | 1.7 | 7.0±0.47 | 0.66±0.039 |

[1]SUVA = specific ultraviolet absorbance; [2]The assimilable organic carbon (AOC) utilized by the indigenous microbial community in each water sample; [3]The assimilable organic carbon (AOC) utilized by strain KN65.2 in each water sample.

## REFERENCES

(1) Benner, J.; Helbling, D. E.; Kohler, H. P. E.; Wittebol, J.; Kaiser, E.; Prasse, C.; Ternes, T. A.; Albers, C. N.; Aamand, J.; Horemans, B.; Springael, D.; Walravens, E.; Boon, N., Is biological treatment a viable alternative for micropollutant removal in drinking water treatment processes? *Water Res.* **2013,** *47*, (16), 5955-5976.

(2) Fenner, K.; Canonica, S.; Wackett, L. P.; Elsner, M., Evaluating pesticide degradation in the environment: blind spots and emerging opportunities. *Science* **2013,** *341*, (6147), 752-758.

(3) Moschet, C.; Wittmer, I.; Simovic, J.; Junghans, M.; Piazzoli, A.; Singer, H.; Stamm, C.; Leu, C.; Hollender, J., How a complete pesticide screening changes the assessment of surface water quality. *Environ. Sci. Technol.* **2014,** *48*, (10), 5423-5432.

(4) Sekhar, A.; Horemans, B.; Aamand, J.; Sorensen, S. R.; Vanhaecke, L.; Vanden Bussche, J.; Hofkens, J.; Springael, D., Surface colonization and activity of the 2,6-Dichlorobenzamide (BAM) degrading aminobacter sp strain MSH1 at macro- and micropollutant BAM concentrations. *Environ. Sci. Technol.* **2016,** *50*, (18), 10123-10133.

(5) Nguyen, T. P. O.; Helbling, D. E.; Bers, K.; Fida, T. T.; Wattiez, R.; Kohler, H. P. E.; Springael, D.; De Mot, R., Genetic and metabolic analysis of the carbofuran catabolic pathway in Novosphingobium sp KN65.2. *Appl. Microbiol. Biotechnol.* **2014,** *98*, (19), 8235-8252.

(6) Owsianiak, M.; Dechesne, A.; Binning, P. J.; Chambon, J. C.; Sorensen, S. R.; Smets, B. F., Evaluation of bioaugmentation with entrapped degrading cells as a soil remediation technology. *Environ. Sci. Technol.* **2010,** *44*, (19), 7622-7627.

(7) Scheutz, C.; Broholm, M. M.; Durant, N. D.; Weeth, E. B.; Jorgensen, T. H.; Dennis, P.; Jacobsen, C. S.; Cox, E. E.; Chambon, J. C.; Bjerg, P. L., Field evaluation of biological enhanced

reductive dechlorination of chloroethenes in clayey till. *Environ. Sci. Technol.* **2010,** *44*, (13), 5134-5141.

(8) Haig, S. J.; Gauchotte-Lindsay, C.; Collins, G.; Quince, C., Bioaugmentation mitigates the impact of estrogen on coliform-grazing protozoa in slow sand filters. *Environ. Sci. Technol.* **2016,** *50*, (6), 3101-3110.

(9) Albers, C. N.; Feld, L.; Ellegaard-Jensen, L.; Aamand, J., Degradation of trace concentrations of the persistent groundwater pollutant 2,6-dichlorobenzamide (BAM) in bioaugmented rapid sand filters. *Water Res.* **2015,** *83*, 61-70.

(10) Helbling, D. E.; Hammes, F.; Egli, T.; Kohler, H. P. E., Kinetics and yields of pesticide biodegradation at low substrate concentrations and under conditions restricting assimilable organic carbon. *Appl. Environ. Microbiol.* **2014,** *80*, (4), 1306-1313.

(11) Egli, T., How to live at very low substrate concentration. *Water Res.* **2010,** *44*, (17), 4826-4837.

(12) Hammes, F. A.; Egli, T., New method for assimilable organic carbon determination using flow-cytometric enumeration and a natural microbial consortium as inoculum. *Environ. Sci. Technol.* **2005,** *39*, (9), 3289-3294.

(13) Vital, M.; Hammes, F.; Egli, T., Escherichia coli O157 can grow in natural freshwater at low carbon concentrations. *Environ. Microbiol.* **2008,** *10*, (9), 2387-2396.

(14) Horemans, B.; Vandermaesen, J.; Breugelmans, P.; Hofkens, J.; Smolders, E.; Springael, D., The quantity and quality of dissolved organic matter as supplementary carbon source impacts the pesticide-degrading activity of a triple-species bacterial biofilm. *Appl. Microbiol. Biotechnol.* **2014,** *98*, (2), 931-943.

(15) Zhang, W. L.; Li, Y.; Wang, C.; Wang, P. F.; Hou, J.; Yu, Z. B.; Niu, L. H.; Wang, L. Q.; Wang, J., Modeling the Biodegradation of Bacterial Community Assembly Linked Antibiotics in River Sediment Using a Deterministic Stochastic Combined Model. *Environ. Sci. Technol.* **2016,** *50*, (16), 8788-8798.

(16) Song, D. J.; Kitamura, M.; Katayama, A., Approach for Estimating Microbial Growth and Biodegradation of Hydrocarbon Contaminants in Subsoil Based on Field Measurements: 2. Application in a Field Lysimeter Experiment. *Environ. Sci. Technol.* **2010,** *44*, (17), 6795-6801.

(17) Vital, M.; Hammes, F.; Egli, T., Competition of Escherichia coli O157 with a drinking water bacterial community at low nutrient concentrations. *Water Res.* **2012,** *46*, (19), 6279-6290.

(18) Van Nevel, S.; De Roy, K.; Boon, N., Bacterial invasion potential in water is determined by nutrient availability and the indigenous community. *FEMS Microbiol. Ecol.* **2013,** *85*, (3), 593-603.

(19) Horemans, B.; Breugelmans, P.; Saeys, W.; Springael, D., Soil-Bacterium Compatibility Model as a Decision-Making Tool for Soil Bioremediation. *Environ. Sci. Technol.* **2017,** *51*, (3), 1605-1615.

(20) Liu, L.; Helbling, D. E.; Kohler, H. P. E.; Smets, B. F., A model framework to describe growth-linked biodegradation of trace-level pollutants in the presence of coincidental carbon substrates and microbes. *Environ. Sci. Technol.* **2014,** *48*, (22), 13358-13366.

(21) Caldas, S. S.; Demoliner, A.; Costa, F. P.; D'Oca, M. G. M.; Primel, E. G., Pesticide residue determination in groundwater using solid-phase extraction and high-performance liquid chromatography with diode array detector and liquid chromatography-tandem mass spectrometry. *J. Braz. Chem. Soc* **2010,** *21*, (4), 642-650.

(22) Chiron, S.; Valverde, A.; FernandezAlba, A.; Barcelo, D., Automated sample preparation for monitoring groundwater pollution by carbamate insecticides and their transformation products. *J. AOAC Int.* **1995,** *78*, (6), 1346-1352.

(23) Chowdhury, M. A. Z.; Banik, S.; Uddin, B.; Moniruzzaman, M.; Karim, N.; Gan, S. H., Organophosphorus and carbamate pesticide residues detected in water samples collected from paddy and vegetable fields of the Savar and Dhamrai Upazilas in Bangladesh. *Int. J. Env. Res. Public Health* **2012,** *9*, (9), 3318-3329.

(24) De Llasera, M. P. G.; Bernal-Gonzalez, M., Presence of carbamate pesticides in environmental waters from the northwest of Mexico: Determination by liquid chromatography. *Water Res.* **2001,** *35*, (8), 1933-1940.

(25) Tariq, M. Y.; Afzal, S.; Hussain, I., Degradation and persistence of cotton pesticides in sandy loam soils from Punjab, Pakistan. *Environ. Res.* **2006,** *100*, (2), 184-196.

(26) Vryzas, Z.; Vassiliou, G.; Alexoudis, C.; Papadopoulou-Mourkidou, E., Spatial and temporal distribution of pesticide residues in surface waters in northeastern Greece. *Water Res.* **2009,** *43*, (1), 1-10.

(27) Helbling, D. E., Bioremediation of pesticide-contaminated water resources: the challenge of low concentrations. *Curr. Opin. Biotechnol.* **2015,** *33*, 142-148.

(28) Eaton, A. D.; Clesceri, L. S.; Franson, M. A. H.; Association, A. P. H.; Greenberg, A. E.; Rice, E. W.; Association, A. W. W.; Federation, W. E., *Standard methods for the examination of water & wastewater*. American Public Health Association: Washington, DC, 2005.

(29) Vital, M.; Füchslin, H. P.; Hammes, F.; Egli, T., Growth of Vibrio cholerae O1 Ogawa Eltor in freshwater. *Microbiology* **2007,** *153*, (7), 1993-2001.

(30) Hammes, F.; Berney, M.; Wang, Y. Y.; Vital, M.; Koster, O.; Egli, T., Flow-cytometric total bacterial cell counts as a descriptive microbiological parameter for drinking water treatment processes. *Water Res.* **2008,** *42*, (1-2), 269-277.

(31) Terada, A.; Lackner, S.; Kristensen, K.; Smets, B. F., Inoculum effects on community composition and nitritation performance of autotrophic nitrifying biofilm reactors with counter-diffusion geometry. *Environ. Microbiol.* **2010,** *12*, (10), 2858-2872.

(32) Walton, N. R. G., Electrical-conductivity and total dissolved solids - what is their precise relationship. *Desalination* **1989,** *72*, (3), 275-292.

(33) Arrieta, J. M.; Mayol, E.; Hansman, R. L.; Herndl, G. J.; Dittmar, T.; Duarte, C. M., Dilution limits dissolved organic carbon utilization in the deep ocean. *Science* **2015,** *348*, (6232), 331-333.

(34) Stegen, J. C.; Johnson, T.; Fredrickson, J. K.; Wilkins, M. J.; Konopka, A. E.; Nelson, W. C.; Arntzen, E. V.; Chrisler, W. B.; Chu, R. K.; Fansler, S. J.; Graham, E. B.; Kennedy, D. W.; Resch, C. T.; Tfaily, M.; Zachara, J., Influences of organic carbon speciation on hyporheic corridor biogeochemistry and microbial ecology. *Nat. Commun.* **2018,** *9*, 585.

(35) Weishaar, J. L.; Aiken, G. R.; Bergamaschi, B. A.; Fram, M. S.; Fujii, R.; Mopper, K., Evaluation of specific ultraviolet absorbance as an indicator of the chemical composition and reactivity of dissolved organic carbon. *Environ. Sci. Technol.* **2003,** *37*, (20), 4702-4708.

(36) Li, C. W.; Benjamin, M. M.; Korshin, G. V., Use of UV spectroscopy to characterize the reaction between NOM and free chlorine. *Environ. Sci. Technol.* **2000,** *34*, (12), 2570-2575.

(37) Ates, N.; Kitis, M.; Yetis, U., Formation of chlorination by-products. in waters with low SUVA-correlations with SUVA and differential UV spectroscopy. *Water Res.* **2007,** *41*, (18), 4139-4148.

528 (38) Escobar, I. C.; Randall, A. A.; Taylor, J. S., Bacterial growth in distribution systems: Effect
529 of assimilable organic carbon and biodegradable dissolved organic carbon. *Environ. Sci. Technol.*
530 **2001,** *35*, (17), 3442-3447.
531 (39) Rosenstock, B.; Zwisler, W.; Simon, M., Bacterial consumption of humic and non-humic low
532 and high molecular weight DOM and the effect of solar irradiation on the turnover of labile DOM
533 in the Southern Ocean. *Microb Ecol* **2005,** *50*, (1), 90-101.
534 (40) Simkins, S.; Mukherjee, R.; Alexander, M., 2 Approaches to modeling kinetics of
535 biodegradation by growing-cells and application of a 2-compartment model for mineralization
536 kinetics in sewage. *Appl. Environ. Microbiol.* **1986,** *51*, (6), 1153-1160.
537 (41) Singh, B. K.; Walker, A.; Morgan, J. A. W.; Wright, D. J., Biodegradation of chlorpyrifos by
538 Enterobacter strain B-14 and its use in bioremediation of contaminated soils. *Appl. Environ.*
539 *Microbiol.* **2004,** *70*, (8), 4855-4863.

540

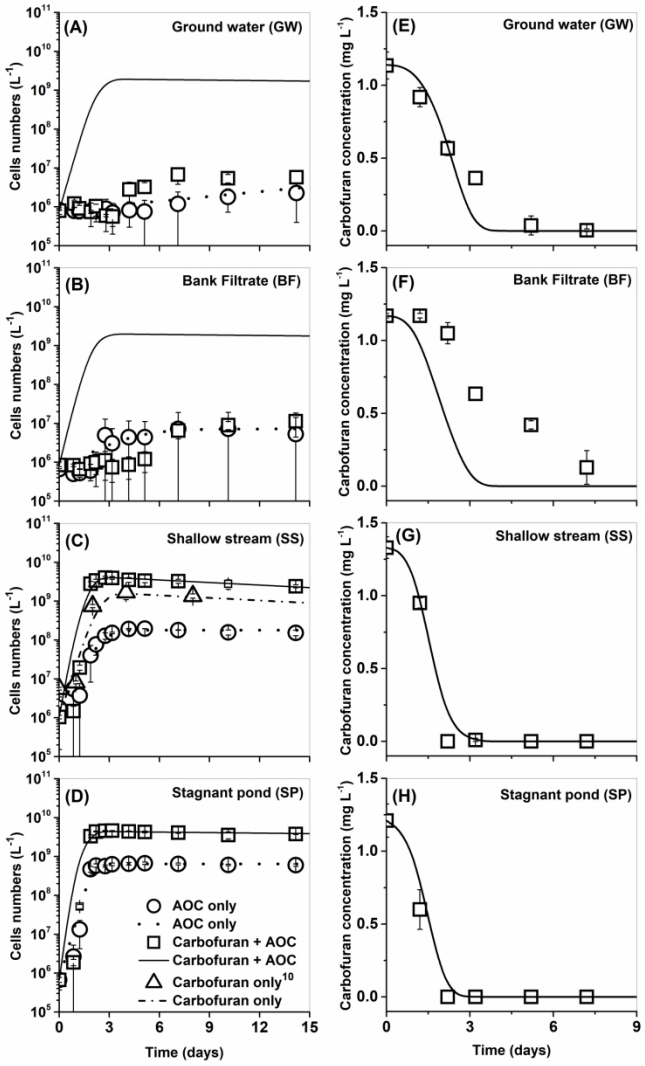


Figure 1. Results from batch experiments (discrete symbols) and model simulations (continuous lines) investigating (A-D) the growth of strain KN65.2 and (E-H) the biotransformation of carbofuran. We report the growth of KN65.2 only on residual AOC (circles; dotted lines) and on carbofuran in the presence of residual AOC (squares; solid line) in different water samples. The growth of KN65.2 on carbofuran in AOC-restricted mineral media (data from Helbling et al 10 in triangles and fitted with dot-dashed line) is shown in figure C. We report biotransformation of carbofuran in the presence of residual AOC for different water samples (E-H).

99x149mm (600 x 600 DPI)

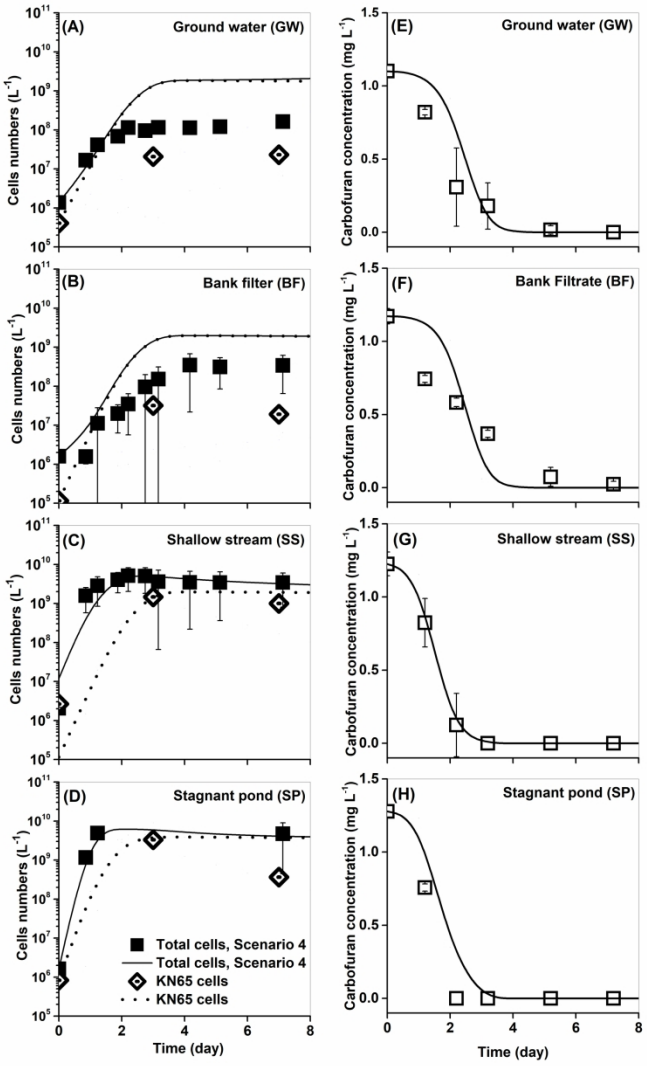


Figure 2. Results from batch experiments (discrete symbols) and model simulations (continuous lines) investigating (A-D) the growth of the combined microbial community (strain KN65.2 + indigenous microbial community) and the growth of strain KN65.2 and (E-H) the biotransformation of carbofuran. We report the combined microbial community on carbofuran in the presence of residual AOC (filled square; solid line), and KN65.2 on carbofuran in the presence of residual AOC and the indigenous microbial community (diamonds; dotted line) for different water samples. We report biotransformation of carbofuran in the presence of residual AOC and the indigenous microbial community for different water samples (E-H).

99x148mm (600 x 600 DPI)

# Modelling carbofuran biotransformation by *Novosphingobium* sp. KN65.2 in the presence of coincidental carbon and indigenous microbes

*Li Liu[1,2†], Damian E. Helbling[3,4*†], Hans-Peter E. Kohler[3], Barth F. Smets[1]**

[1]Department of Environmental Engineering, Technical, University of Denmark, Bygningstorvet 115, 2800 Kgs. Lyngby, Denmark;

[2]School of Chemistry, Beihang University, Beijing 100191, P. R. China;

[3]Eawag, Swiss Federal Institute of Aquatic Science and Technology, Department of Environmental Microbiology, Überlandstrasse 133, 8600 Dübendorf, Switzerland;

[4]School of Civil and Environmental Engineering, Cornell University, Ithaca, NY, USA.

***Corresponding authors:**

bfsm@env.dtu.dk, phone: +45 45 25 22 30, fax: +45 45 93 28 50

damian.helbling@cornell.edu, phone: +1 607 255 5146, fax: +1 607 255 9004

**†These authors contributed equally to this work**

# of pages: 5

# of tables: 2

# of figures: 2

**TABLE S1.** Matrix notation of the model framework.

| | | V1 | V2 | V3 | V4 | V5 | Kinetics Rate Expression |
|---|---|---|---|---|---|---|---|
| | | $S_{TP}$ | $S_{AOC,X}$ | $S_{AOC,other}$ | $X_{KN65.2}$ | $X_{BC}$ | |
| **$X_{KN65.2}$** | | | | | | | |
| P1 | Growth $X_{KN65.2}$ on $S_{TP}$ | $-\frac{1}{Y_{TP,X}}$ | | | 1 | | $\mu_{XB,X,TP,max}\frac{S_{TP}X_{KN65.2}}{S_{TP}+K_{TP,X}}$ |
| P2 | Growth $X_{KN65.2}$ on $S_{AOC,Z}$ | | $-\frac{1}{Y_{AOC,X}}$ | | 1 | | $\mu_{XB,X,AOC,max}\frac{S_{AOC,X}X_{KN65.2}}{S_{AOC,X}+K_{AOC,X}}$ |
| P3 | Decay of $X_{KN65.2}$ | | | | -1 | | $b_X X_{KN65.2}$ |
| **$X_{BC}$** | | | | | | | |
| P4 | Growth $X_{BC}$ on $S_{AOC,X}$ | | $-\frac{1}{Y_{AOCX,BC}}$ | | | 1 | $\mu_{XB,BC,AOCx,max}\frac{S_{AOC,X}X_{BC}}{S_{AOC,X}+K_{AOC,X,BC}}$ |
| P5 | Growth $X_{BC}$ on $S_{AOC,other}$ | | | $-\frac{1}{Y_{AOCother,BC}}$ | | 1 | $\mu_{XB,BC,AOC\ other,max}\frac{S_{AOC,other}X_{BC}}{S_{AOC,other}+K_{AOC,other,BC}}$ |
| P6 | Decay of $X_{BC}$ | | | | | -1 | $b_{BC}X_{BC}$ |

**TABLE S2.** Model parameters calculated from batch experiments in the absence of carbofuran supplements.

| ***Strain*** | **KN65 ($X_{KN65}$)** | | | | | **Natural community ($X_{BC}$)** | | | |
|---|---|---|---|---|---|---|---|---|---|
| **Substrate** | **Carbofuran[1]** | **$AOC_{GW}$** | **$AOC_{BF}$** | **$AOC_{SS}$** | **$AOC_{SP}$** | **$AOC_{GW}$** | **$AOC_{BF}$** | **$AOC_{SS}$** | **$AOC_{SP}$** |
| $\mu_{max}$ [$day^{-1}$] | 7.8 | 0.106 | 0.647 | 7.78 | 15.18 | 10.0 | 10.11 | 16.78 | 6.11 |
| $K_s$ [mg $L^{-1}$] | 1.5 | 0.0001 | $1.4\times10^{-4}$ | 0.63 | 1.92 | 4.35 | 1.10 | 2.64 | 0.0003 |
| $Y_{C/S}$ [Cells (mg substrate)$^{-1}$] | $3.12\times10^{9}$ | $1.0\times10^{9}$ | $1.0\times10^{9}$ | $1.0\times10^{9}$ | $1.0\times10^{9}$ | $1.0\times10^{9}$ | $1.0\times10^{9}$ | $1.0\times10^{9}$ | $1.0\times10^{9}$ |

[1]Data from previous publication: Helbling, D. E.; Hammes, F.; Egli, T.; Kohler, H. P. E., Kinetics and Yields of Pesticide Biodegradation at Low Substrate Concentrations and under Conditions Restricting Assimilable Organic Carbon. *Appl Environ Microb* 2014, 80, (4), 1306-1313.

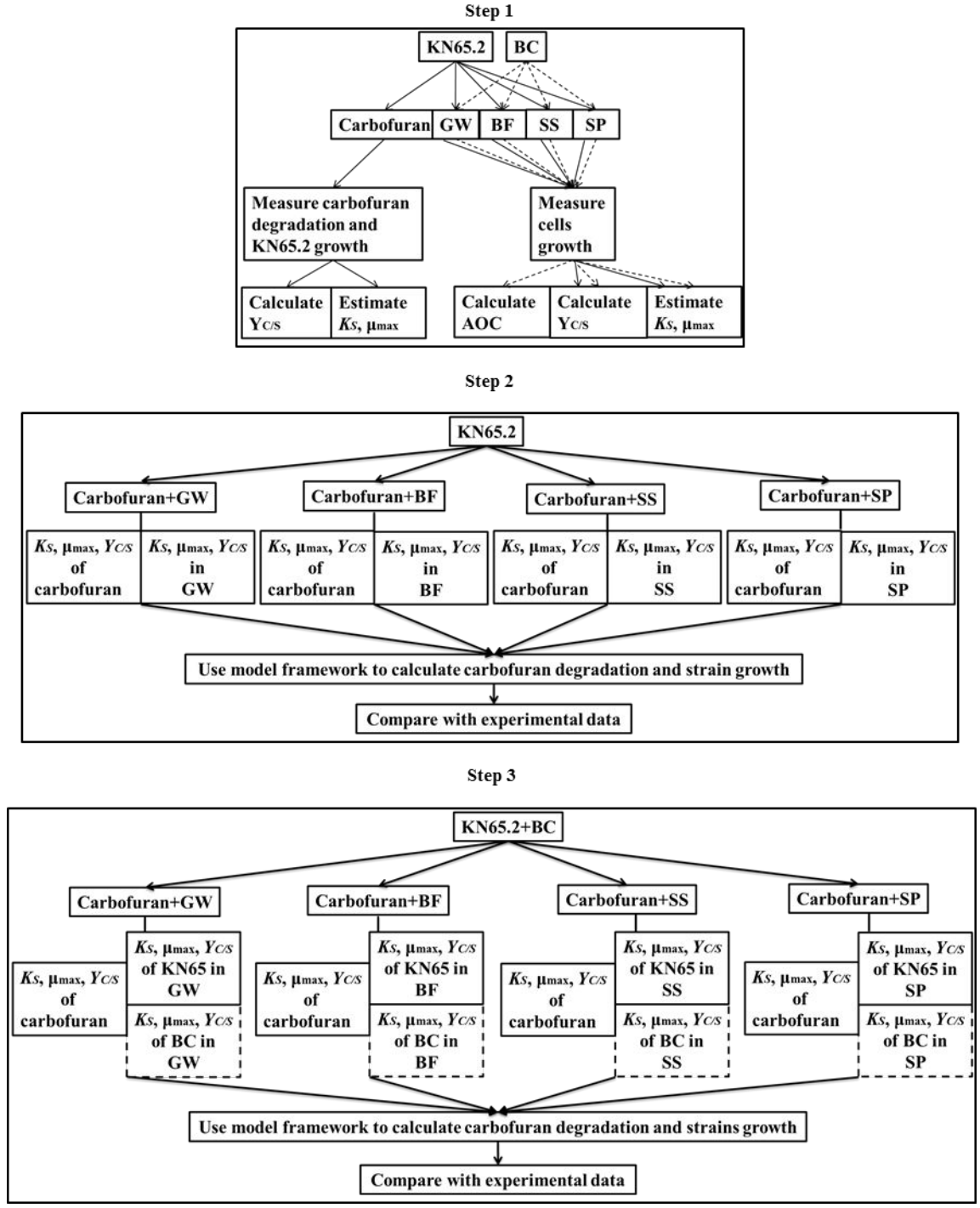


**FIGURE S1.** General procedure for prediction of carbofuran degradation by KN65.2 in water samples by the proposed model framework

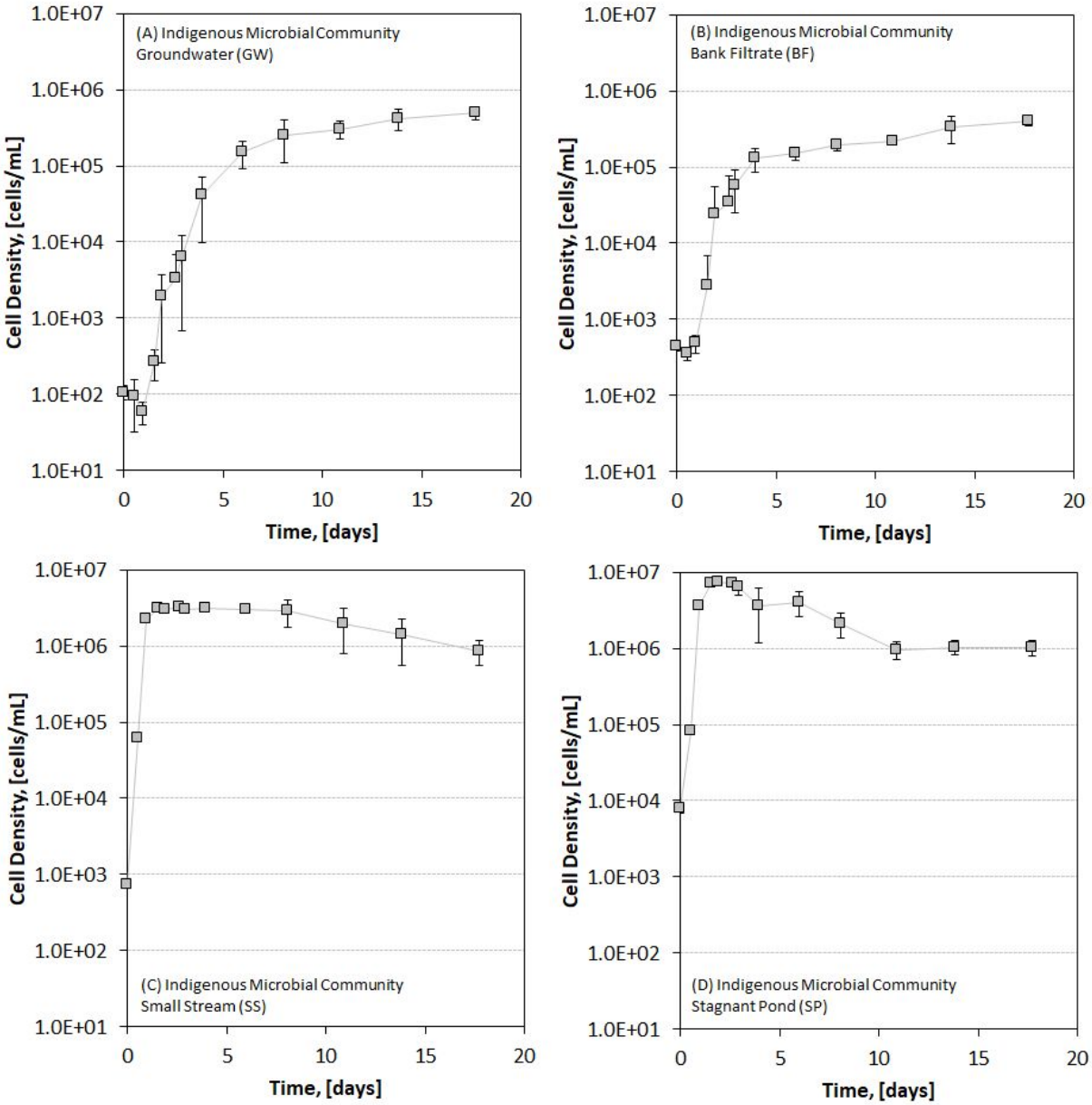


**Figure S2:** Growth of the indigenous microbial community on AOC in (A) groundwater, (B) bank filtrate, (C) a shallow stream, and (D) a stagnant pond.

## TOC Graphic

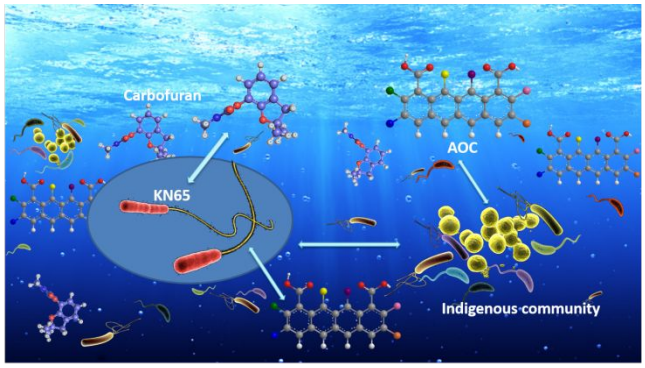


## TOC Entry

Interference of coincidental carbon and indigenous bacteria on pesticide removal by biodegrading strains differs in low *versus* high AOC waters.